
Masters Theses


Student Theses and Dissertations

Summer 2017

Cathodic protection measurement through inline inspection technology uses and observations

Briana Ley Ferguson

Follow this and additional works at: https://scholarsmine.mst.edu/masters_theses

 Part of the [Chemical Engineering Commons](#), [Materials Science and Engineering Commons](#), and the [Mechanical Engineering Commons](#)

Department:

Recommended Citation

Ferguson, Briana Ley, "Cathodic protection measurement through inline inspection technology uses and observations" (2017). *Masters Theses*. 7690.

https://scholarsmine.mst.edu/masters_theses/7690

This thesis is brought to you by Scholars' Mine, a service of the Missouri S&T Library and Learning Resources. This work is protected by U. S. Copyright Law. Unauthorized use including reproduction for redistribution requires the permission of the copyright holder. For more information, please contact scholarsmine@mst.edu.

CATHODIC PROTECTION MEASUREMENT THROUGH INLINE INSPECTION
TECHNOLOGY USES AND OBSERVATIONS

by

BRIANA LEY FERGUSON

A THESIS

Presented to the Faculty of the Graduate School of the
MISSOURI UNIVERSITY OF SCIENCE AND TECHNOLOGY

In Fulfillment of the Requirements for the Degree

MASTER OF SCIENCE IN MECHANICAL ENGINEERING

2017

Approved by

Dr. Matthew J. O'Keefe, Co-Advisor

Dr. Victor Birman, Co-Advisor

Dr. James Drewniak, Committee Member

© 2017

Briana Ley Ferguson

All Rights Reserved

ABSTRACT

This research supports the evaluation of an impressed current cathodic protection (CP) system of a buried coated steel pipeline through alternative technology and methods, via an inline inspection device (ILI, CP ILI tool, or tool), in order to prevent and mitigate external corrosion. This thesis investigates the ability to measure the current density of a pipeline's CP system from inside of a pipeline rather than manually from outside, and then convert that CP ILI tool reading into a pipe-to-soil potential as required by regulations and standards. This was demonstrated through a mathematical model that utilizes applications of Ohm's Law, circuit concepts, and attenuation principles in order to match the results of the ILI sample data by varying parameters of the model (i.e., values for over potential and coating resistivity). This research has not been conducted previously in order to determine if the protected potential range can be achieved with respect to the predicted current density from the CP ILI device. Kirchhoff's method was explored, but certain principals could not be used in the model as manual measurements were required. This research was based on circuit concepts which indirectly affected electrochemical processes. Through Ohm's law, the results show that a constant current density is possible in the protected potential range; therefore, indicates polarization of the pipeline, which leads to calcareous deposit development with respect to electrochemistry. Calcareous deposit is desirable in industry since it increases the resistance of the pipeline coating and lowers current, thus slowing the oxygen diffusion process. This research conveys that an alternative method for CP evaluation from inside of the pipeline is possible where the pipe-to-soil potential can be estimated (as required by regulations) from the ILI tool's current density measurement.

ACKNOWLEDGMENTS

I am grateful for my professors, Dr. O’Keefe, Dr. Birman, and Dr. Drewniak, for helping me move forward and make this interesting study possible. These gentlemen are very serious, knowledgeable, positive, as well as approachable. I liked my professors’ professionalism, leadership, and openness for ideas with respect real world engineering and collaborations with subject matter experts (SMEs). I am fortunate for the education and opportunity Missouri S&T provided to do this study remotely through use of technology to facilitate collaborations.

Thank you Dr. Birman for introducing me to Dr. O’Keefe! I am especially thankful and value industry connections made through Dr. O’Keefe like Mr. Mark Mateer, Principle Asset Integrity Engineer from Shell, who became a key figure for this study and a great mentor. Mark helped me establish important connections with other serious supporters (mentors) such as Mr. David Williams, CP Specialist (NACE CP4), from Baker Hughes. Also thanks to resources and teachers like Mr. Joe Pikas, VP of Pipeline Integrity & Corrosion Engineering, from Technical Toolboxes. Thank you all for the wonderful material, guidance, and assistance.

Thank you to my dearest friend, Mr. Alex B. Fernandez, for encouraging me to keep pushing forward with my dreams and endeavors.

TABLE OF CONTENTS

	Page
ABSTRACT.....	iii
ACKNOWLEDGMENTS	iv
LIST OF ILLUSTRATIONS.....	viii
LIST OF TABLES.....	xi
NOMENCLATURE	xii
 SECTION	
1. INTRODUCTION	1
1.1. RESEARCH OBJECTIVE	1
1.2. BACKGROUND	3
1.2.1. External Corrosion Background.....	3
1.2.1.1 Types of corrosion of steel pipelines	3
1.2.1.2 Ferrous steel corrosion.....	4
1.2.1.3 Diffusion – Fick’s Law.....	7
1.2.2. Corrosion Cell Components.....	10
1.2.3. Cathodic Protection Background.....	12
1.2.3.1 Brief history of CP.....	12
1.2.3.2 Cathodic protection -general design and use.....	13
1.2.3.3 CP and attenuation	15
1.2.3.4 CP and calcareous deposit relationship.....	15
1.2.4. Regulatory Requirements for CP.....	19
1.2.5. Use of ILI Tool for CP Measurement.....	20

1.3. INTRODUCTION TO THE CP ILI TOOL.....	22
2. ENGINEERING ANALYSIS & METHODOLOGY	27
2.1. PROBLEM APPROACH	27
2.2. ASSUMPTIONS.....	28
2.3. CP ANALYSIS.....	30
2.4. ATTENUATION of CURRENT & POTENTIAL.....	33
2.5. ANALYTICAL VIEW PER CP ILI.....	36
2.6. KIRCHHOFF'S & OHM'S LAW for CORROSION CELL	38
2.6.1. Circuit of General CP System.	40
2.6.2. Circuit of CP System with ILI Inside of Pipeline.	43
3. CP ILI DATA & MODEL RESULTS.....	46
3.1. DATA FROM CP ILI TOOL	46
3.1.1. CP ILI Data Set #1.....	46
3.1.2 CP ILI Data Set #2.....	48
3.1.3. CP ILI Data Set #3.....	49
3.2. MODEL RESULTS PER ENGINEERING ANALYSIS ON CP ILI DATA	51
3.2.1. Constant Over Potential and Varied Coating Resistivity	52
3.2.2. Varied Over Potential And Constant Coating Resistivity.....	58
4. DISCUSSIONS AND CONCLUSIONS	65
4.1. DISCUSSION – RESULTS OF GRAPHS & CHARTS.....	65
4.2. FINDINGS.....	70
4.3. CONCLUSIONS.....	72

4.4. FUTURE WORK.....	73
4.4.1. Calcareous Deposit.....	74
4.4.2. Kirchhoff's Theory Applications.	74
4.4.3. Diffusion Rate Experiments.	74
4.4.4. Noise and Vibration Filter.....	75
4.4.5. Sensor Types and Arrangements.....	75
4.4.6. Non-Surface-Contact Sensors.	75
APPENDICES	
A.MISCELLANEOUS TABLES & MATERIALS	76
B.LITERATURE & PATENT REVIEW	80
C.OTHER REFERENCES & MATERIAL.....	83
BIBLIOGRAPHY.....	86
VITA.....	89

LIST OF ILLUSTRATIONS

	Page
Figure 1.1 – Tafel Plot, Rotating Cylinder Test.....	7
Figure 1.2 – Concept of Protected Pipe, Potential vs. Natural Log of Current	8
Figure 1.3 – Lazzari and Pedferri – Polarization Diagram of Iron	10
Figure 1.4 – Diagram of CP with R = Rectifier, and Current Flow.....	11
Figure 1.5 – Part 1, Calcareous Deposit Example –Shrink Sleeve & Coating Interface..	16
Figure 1.6 – Part 2, Calcareous Deposit Example –Shrink Sleeve & Coating Interface ¹²	17
Figure 1.7 – Image Redrawn from “Cathodic Protection” –Lazzari & Pediferri ¹	19
Figure 1.8 – Baker Hughes Public Video www.BakerHughes.com ¹⁴	23
Figure 1.9 – CP ILI Within the Pipe Conceptualization.....	24
Figure 2.1 – Pipeline Schematic for Analysis ¹	31
Figure 2.2 – Pipeline Schematic, Redrawn Relating to Figure 2.1 for Analysis ¹	32
Figure 2.3 – Attenuation Trends for Current and Potential	33
Figure 2.4 – Tool Reading - Sensor Contact Points 1 & 2 (Parts a. & b.).....	38
Figure 2.5 – Circuit Diagram of Cathodically Protected Pipe (a.).....	42
Figure 2.6 – Circuit Diagram of Cathodically Protected Pipe (b.)	42
Figure 2.7 –Circuit Diagram of CP Pipe with ILI Measurement from Inside	43
Figure 3.1 – CP ILI Sample Data Set 1, Plot.....	47
Figure 3.2 – CP ILI Sample Data Set 2, by Every 10cm.....	49
Figure 3.3 – CP ILI Sample Data Set 3, by Every 10cm	50
Figure 3.4 – Current Flow and E-field Conceptualization (Parts a. & b.)	51
Figure 3.5 – Cathode ΔE_x Atten. @ Constant -100mV E_L (Data Set#1).....	52

Figure 3.6 – Predicted ΔI_x at Constant E_L (Data Set#1)	53
Figure 3.7 – Cathode ΔE_x Atten. @ Constant -100mV E_L (Data Set#2a)	53
Figure 3.8 – Predicted ΔI_x at Constant E_L (Data Set#2a).....	54
Figure 3.9 – Cathode ΔE_x Atten. @ Constant -100mV E_L (Data Set#2b).....	54
Figure 3.10 – Predicted Current Density at Constant E_L (Data Set#2b).....	55
Figure 3.11 – Cathode ΔE_x Atten. @ Constant -100mV E_L (Data Set#2c).....	55
Figure 3.12 – Predicted ΔI_x at Constant E_L (Data Set#2c).....	56
Figure 3.13 – Cathode ΔE_x Atten. @ Constant -100mV E_L (Data Set#3a)	56
Figure 3.14 – Predicted ΔI_x at Constant E_L (Data Set#3a).....	57
Figure 3.15 – Cathode ΔE_x Atten. @ Constant -100mV E_L (Data Set#3b).....	57
Figure 3.16 – Predicted ΔI_x at Constant E_L (Data Set#3b)	58
Figure 3.17 – Cathode ΔE_x Atten. at Varied E_L (Data Set#1)	59
Figure 3.18 – Predicted ΔI_x @ Constant Coating Resistivity (Data Set#1).....	59
Figure 3.19 – Cathode ΔE_x Atten. at Varied E_L (Data Set#2a).....	60
Figure 3.20 – Predicted ΔI_x @ Constant Coating Resistivity (Data Set#2a).....	60
Figure 3.21 – Cathode ΔE_x Atten. at Varied E_L (Data Set#2b).....	61
Figure 3.22 – Predicted ΔI_x @ Constant Coating Resistivity (Data Set#2b).....	61
Figure 3.23 – Cathode ΔE_x Atten. at Varied E_L (Data Set#2c).....	62
Figure 3.24 – Predicted ΔI_x @ Constant Coating Resistivity (Data Set#2c).....	62
Figure 3.25 – Cathode ΔE_x Atten. at Varied E_L (Data Set#3a).....	63
Figure 3.26 – Predicted ΔI_x @ Constant Coating Resistivity (Data Set#3a).....	63
Figure 3.27 – Cathode ΔE_x Atten. at Varied E_L (Data Set#3b).....	64
Figure 3.28 – Predicted ΔI_x @ Constant Coating Resistivity (Data Set#3b).....	64

Figure 4.1 – Conceptualization of Data Observations	66
Figure 4.2 – Table 3.1 ΔI_x & $\Delta \Psi_x$ as Coating Resistivity Increases.....	68
Figure 4.3 – Magnification of $\Delta \Psi_x$ mV (Fig. 4.2) as Coating Resistivity Increases	68
Figure 4.4 – From Table 3.2 Data: ΔI_x & $\Delta \Psi_x$ Driven by $\Delta \Psi_L$	69
Figure 4.5 – Current Density at Drain Point and Normalized Current	72

LIST OF TABLES

	Page
Table 3.1 – List of CP ILI Data Sets with Sample Reading Size per Distance	46
Table 4.1 – Constant Over Potential ($\Psi_L = \Delta E_L$), “Midpoint” Voltage	67
Table 4.2 – Constant Coating Resistivity Ωm	69

NOMENCLATURE

Symbol	Description
a_m	Reaction quotient
a_{att}	Attenuation constant $(R_4/R_k)^{0.5}$
Amp or A	Ampere, unit of measure for current = C/sec
C	Coulomb
C	Chemical elemental name from nonmetal noble gases for carbon
Ca	Chemical elemental name from main group metals for calcium
CP	Cathodic Protection
D	Diffusion coefficient (diffusivity)
e	base of natural logarithm = 2.718
E or Ψ or Φ	All symbols denote Potential
E_{eq}	Potential Equilibrium, chemical oxidation- reduction is in equilibrium
E°	Standard cell potential
ΔE or Ψ	Change or Drop in Potential
F	Faraday constant 9.6485309×10^4 J/Volt*mol
Fe	Chemical elemental name from transition metals group for (ferrous) Iron
ft	English unit of "foot" representative for length
H	Chemical elemental name from noble gases group for Hydrogen
HS&E	Health, Safety, and Environment (a.k.a. EH&S)
I	Current in general amp
ID	Inner (inside) Diameter
J	Current Density Amp/m ²

J_N	Rate of Diffusion m^2/sec
k	Conductivity coefficient $\Omega*m^{-1}$ (the inverse of resistivity)
L	Length (distance)
L&P	Lazzari & Pedeferrri (Cathodic Protection -Attenuation Methods)
m	Meter
milli	Milli (10^{-3})
Mg	Chemical elemental name from main group metals for Magnesium
μ	Micro (10^{-6})
O	Chemical elemental name for Oxygen
OD	Outer (outside) diameter
Ω	Ohm, a unit of measure of resistance
pH	the electrolytic acidity or basicity of an aqueous solution (corrosiveness)
ρ	resistivity Ωm (the inverse of conductivity)
r	radius of pipe, subscripts denote inner or outer radii of pipe
R_k	Characteristic resistance of the steel pipe
R_u	Universal Gas constant 8.314 (J/mol*K)
R_o	Resistance of coating
R_1	Resistance of leads from rectifier
R_2	Resistance of leads to anode bed
R_3	Resistance of anode bed electrolyte
R_4	Resistance of pipeline ($L_p*R/unit\ length$)
R_5	Resistance of ILI (CP ILI tool)
V	Voltage or volts, unit of measure for potential charge Amp-Ohm ($Amp\Omega$)

1. INTRODUCTION

1.1. RESEARCH OBJECTIVE

This study investigates the ability to convert current flow data collected via an inline inspection (ILI or smart pig) device of a cathodic protection (CP) system of a below ground pipeline into an estimate of pipe-to-soil interface potential (voltage). The supporting physics will utilize Ohm's law, attenuation, electrochemical principles, and Kirchhoff's method. This research and supporting analysis has not been conducted before and would be a benefit to the pipeline industry to help determine and evaluate the effectiveness and consistency of a CP system. This study solely targets the idea to demonstrate the existence of adequate pipe-to-soil potential from the ILI data which results in the development of calcareous deposit on a pipe coating surface. In industry calcareous deposit is an indication that a pipeline is cathodically protected and thus aids with mitigation and prevention of external corrosion as required by regulations.

The research in this document utilizes available studies and knowledge from specialized industry areas and then applying those disciplined areas within the analysis enabling correlation with ILI tool data. This is a multidisciplinary topic including chemistry, corrosion, metallurgy, material science (solid state physics), and electrostatics, where their interrelationships are quite extensive and specialized, hence accessing knowledge and experience of subject matter experts (SMEs) and the developers of the ILI tool. This research will not attempt to prove physical theories or derivations; but rather, it will summarize applications of the already available material. With the aforementioned disciplines many parameters remain to be explored on this topic, with the intent to pave the way for future research.

This thesis is not about providing complete proofs or detailed derivations; rather it briefly summarizes and extends applications of already established methods¹ that are used to evaluate the data from the CP ILI tool. Evaluation of CP systems' effectiveness is mandated by regulations. CP is used to prevent corrosion in order to avoid possible failure and prolong the life of buried or submerged metallic structures. While in general the problem of current density measurement on a steel surface is still unsolved, there is a new method to measure current density for the special case of pipelines. A new ILI tool called the CPCM ToolTM was jointly developed by Baker Hughes Inc. and Shell Projects & Technology to measure current density. There are other similar tools used in industry for vertical down-hole drilling, but this ILI is new to horizontal buried pipelines.

The tool measures current flow from the CP system from inside the pipe as a moving ILI device. This is different from the typical manual measurement of the pipe-to-soil cathode potential from outside of the pipe. The device presents internal automated high-speed current measurement versus external manual low speed potential measurement. This study is intended to show how the two techniques can be related to each other, which has not yet been done in any other study, by showing that pipe potential can be determined from the current density data using basic electrochemistry, Ohm's Law, attenuation, and Kirchhoff's theory.

Pipeline industry-specific audiences for this paper span several applied sciences, technical, and engineering disciplines. Some of the specific disciplines are the following: metallurgy, materials science, structural, corrosion, electrochemical, mechanical, electrical circuitry, and general integrity. Integrity engineering includes various

¹ Lazzari, L.; Pedeferra, P. (2006); "Cathodic protection" (1st Edition). Polipress, Politecnico di Milano Piazza Leonardo da Vinci, 32-20133 Milano.

disciplines for the pipeline system in its entirety, its design, maintenance, and safety, as well as regulatory code compliance.

If sufficient pipe-to-soil potential can be determined from the current density data using basic electrochemistry and the aforementioned electrodynamics, it would expand the practice of CP and benefit the industry by providing a new way to validate regulatory compliance without manually gathering potential data.

1.2. BACKGROUND

To add clarity to the research objective above, the following topics need to be understood and defined in this background before providing a more detailed introduction about the CP ILI tool, discussing applications of related engineering methodologies or any modeled results, and the benefits that this technology brings to industry.

- External Corrosion: Types of Corrosion, Ferrous steel Corrosion, & Diffusion;
- Corrosion Cell Components;
- CP: history, general design, relationships with attenuation & calcareous deposit;
- Regulatory Requirements; and
- Beneficial Use of the CP ILI tool for CP Measurement.

1.2.1. External Corrosion Background. This section describes the different kinds of external corrosion that are relevant to steel pipelines and the specific electrochemical background of ferrous steel corrosion.

1.2.1.1 Types of corrosion of steel pipelines. “Basically, there are four ways corrosion can occur. Corrosion can occur through a chemical reaction or three general types of electrochemical reactions. The three general types of electrochemical reactions that occur depend on the cause of the potential difference between the anode and the

cathode. This potential difference can be caused by differences in the environment, differences in the metal, or by external electrical sources of DC (direct current) current. Understanding this principle leads to an understanding of the principles of operation of CP systems. These three types of corrosion are:

- 1) Concentration cell corrosion
(electrochemical cell caused by differences in the electrolyte),
- 2) Galvanic corrosion
(electrochemical cell caused by differences in the metal), and
- 3) Stray current corrosion
(electrochemical cell caused by external electrical sources).

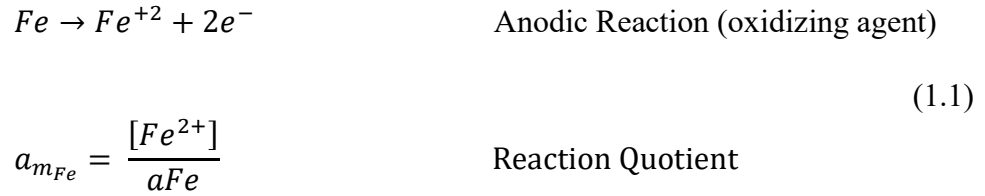
Lastly there is general corrosion; this type of corrosion is either chemical or electrochemical in nature. However, there are no discrete anode or cathode areas. This form of corrosion is uniform over the surface of the metal exposed to the environment. The metal gradually becomes thinner and eventually fails.”²

1.2.1.2 Ferrous steel corrosion. For more context, it is important to understand what general ferrous (iron based, Fe) steel corrosion is and later how CP is designed to mitigate this corrosion. This section and this study will only discuss the simpler aspect for conceptualization of the ferrous steel compound’s oxidation-reduction reaction (corrosion) and ignore other alloy compounds’ electrochemical effects, Equation (1.1).

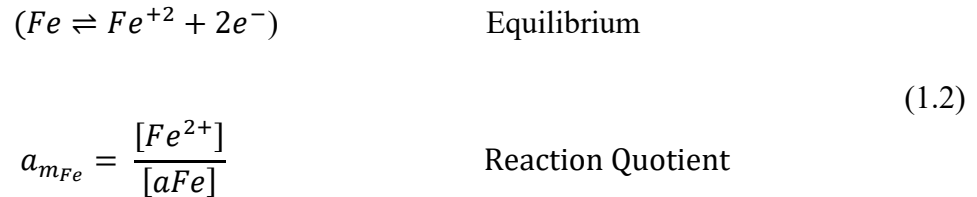
This is demonstrated through standard application of the Gibbs free energy and Nernst methods, Equation (1.4), of electrochemical transformation (reaction) in order to obtain the reduction potential. Observe that the reduction potential is desired to be

² Department of Defence (2003). *Operation and Maintenance: Cathodic Protection*. UFC-3-570-06, Chapter 2-1 (Corrosion Cell), CP Design.

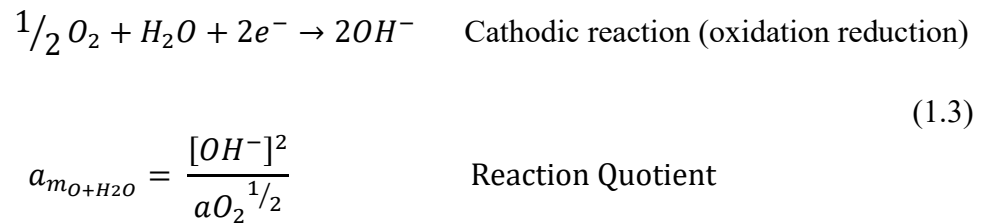
controlled by use of CP as explained later in Section 1.2.3. External corrosion of ferrous steel pipelines consists of the following chemical reactions:



“If the potential at the steel surface is at equilibrium, no corrosion occurs as the reaction rate is equal in both directions (Equation 1.2). The corrosion occurs when the surface potential is more positive than E_{eq} , as shown below (Figure 1.2).”³



“Cathode current plateaus (see Figure 1.1 and Figure 1.2) when the oxygen (O_2) transport to the surface is diffusion limited (Section 1.2.1.3 Diffusion and Figure 1.3). Hydrogen evolution (movement to the surface) occurs if the potential is low and current increases”³ (see Equations 1.3 and 1.6). By the Nernst Equation and Gibbs Free Energy, E_{eq} for the reaction ($Fe \rightleftharpoons Fe^{+2} + 2e^{-}$) is shown below in Equation 1.4.



$$E_{eq} = E^0 - K \ln a_m \quad \text{Nernst Equation; or} \quad (1.4)$$

³ Mateer, M. (2017, April 10). *Background on Corrosion and CP, CPCM Data Analysis Approach* [Telephone interview #1]. Discussions with Mark Mateer, Principal Asset Integrity Engineer.

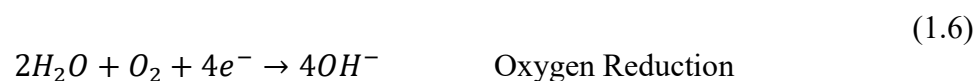
$$\text{At ambient conditions, } E_{eq} = E^o - \frac{0.0257 V}{n} * \ln(a_m)$$

$$\text{Where, } K = \left(\frac{R_u * T}{nF}\right); \text{ and } a_m = \frac{[Products]^n}{[Reactants]^m}$$

$$\text{For equations 1.2 and 1.3 } a_m = \frac{[Fe^{2+}]}{[OH^-]^2}$$

The standard cell potential of the reaction is denoted as E^o , where F is the Faraday constant (9.6485309×10^4 J/V* mol), R_u is the universal gas constant (8.314510 J/K* mol), n is redox number (from oxidation-reduction reaction balanced Equation), T is the absolute temperature (in this case assume ambient at 298 Kelvin for 25°C) and a_m is the ion concentration of the metal (also called the reaction quotient or reaction ratio).⁴

“If electrons can be added, as in Equation (1.5), the reaction of Equation (1.1) can be driven to the left and reduce the reaction rate. If the potential can be driven below E_{eq} then corrosion will stop (Figure 1.2), page 8.”³



The desire is to stop external corrosion (see Figure 1.1 and Figure 1.2) or reduce the rate so much that it becomes insignificant or negligible. This is done electrochemically via the manipulation of the corrosion cell defined in Section 1.2.2 below and through the application of CP design (Section 1.2.3 below and further elaborated on in Section 2.3). The Tafel plot (Figure 1.1) below accompanied by Figure 1.2 shows the potential versus the logarithmic current as seen in the Nernst (1.4) and is

⁴ Kotz, J.; Treichel, P.; (1999) “Chemistry and Chemical Reactivity, Fourth Edition” (Gibbs Free Energy, Standard Potentials, and Electrochemical Cells – Nernst Equation), Chapters: 21 and 20.3; Saunders College Publishing: Fort Worth, TX.

dependent upon the RPM (revolutions per minute) level examples (frequency) due to a rotating cylinder electrode test. “The faster the cylinder spins, the higher the oxygen diffusion rate and the higher the cathode current. The rotation cylinder test also causes the corrosion potential to shift to higher potential where corrosion current has increased, indicating the corrosion rate is higher than when it is at low RPM.”³

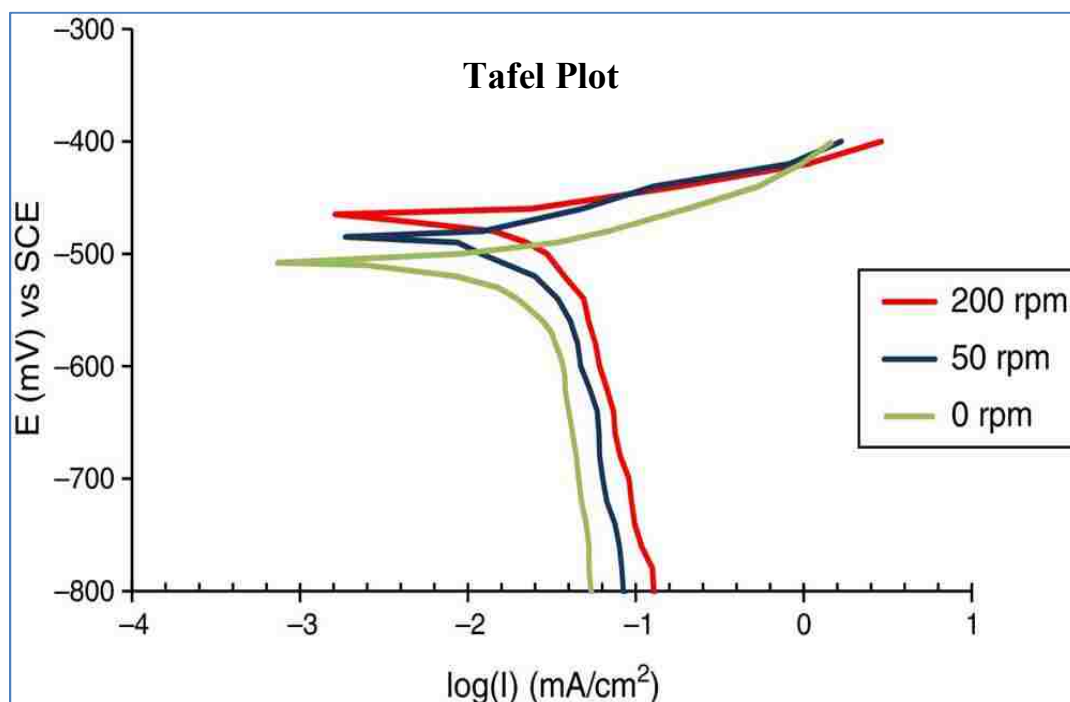


Figure 1.1 –Tafel Plot, Rotating Cylinder Test

1.2.1.3 Diffusion – Fick’s Law. It is important to understand diffusion with respect to electrochemical corrosion of metal. In solid state physics there is a flux of concentration gradient (impurity atoms or vacancies), throughout a solid’s atomic structure represented by Equation (1.7). “In equilibrium the impurities or vacancies will be distributed uniformly. The net flux of J_N of atoms of one species in a solid is related to

the gradient of the concentration N of this species by a phenomenological relation called Fick's Law. To diffuse, an atom must overcome the potential energy barrier presented by its nearest neighbors.”⁵ The “neighbors” are other atoms within the solid's structure. This explanation is basically the lattice bond effects within the metal, where “the gradient of the chemical potential is the driving force for diffusion and not the concentration gradient alone. The number of atoms crossing a unit area per unit time is called the rate of diffusion.”⁵

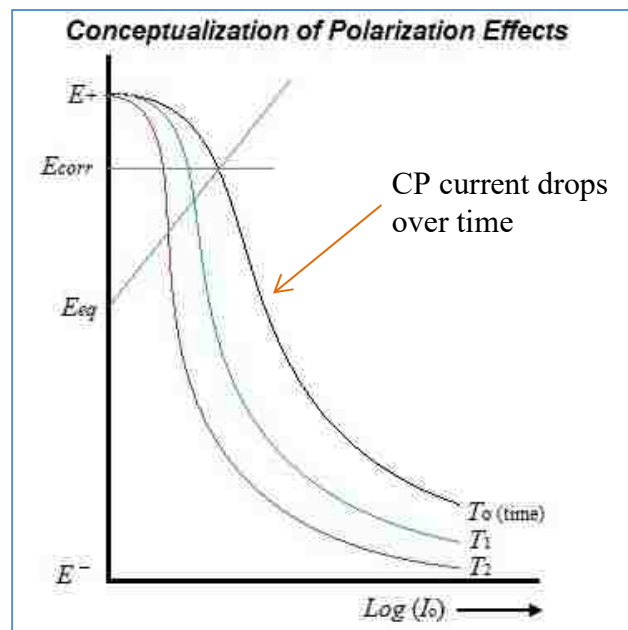


Figure 1.2 – Concept of Protected Pipe, Potential vs. Natural Log of Current

(1.7)

$$J_N = D \nabla N \quad \text{m}^2/\text{sec} = \text{rate of diffusion}$$

-or

⁵ Kittel, C.; (2005), “Introduction to Solid State Physics, Eighth Edition” (Diffusion), Chapters: 20; John Wiley & Sons, Inc.: Hoboken, NJ.

$$J_N = D \nabla N \left(\frac{\Delta c}{\Delta x} \right) \text{ m}^2/\text{sec} = \text{rate of diffusion}$$

$$D = D_0 e^{-E/k_b T}, \quad = \text{diffusion constant or diffusivity} \quad (1.8)$$

Where E in this general case is the activation energy required for the process, k_b is the Boltzmann constant, and T is the absolute temperature. This study assumes constant ambient temperature (ideal, see Section 2.2 for complete list of assumptions), where in industry and experimentally, the temperature can impact the diffusion rate.

Figure 1.3 is the “Polarization diagram of corrosion of iron in aerated aqueous electrolyte.”¹ This model conveys the metal’s process from its original state up to a level of polarization, necessary for articulating electrochemical corrosion concepts and is a more elaborate diagram in relation to the previous Figure 1.2. In this visual model of Figure 1.3 (Potential vs. Current), it helps illustrate that oxygen diffusion (recall Equation 1.6) controls the cathodic reaction and the current will remain constant while the potential varies.

Later in Sections 3, 4 and in Figure 4.1, the results from the CP ILI data and analyses will explain how this applies. Regarding the horizontal E_{corr} line, above it and to the right of the potential curve, is where diffusion takes place (Fick’s law). The diagonal line is E_{eq} (equilibrium from the Nernst Equation) and the triangular space formed between and above the flat E_{corr} and above E_{eq} represents the over potential where the pipe polarizes. Below the E_{appl} and to the right end (tail) of the curve is the hydrogen evolution region. This Figure 1.3 will become an important model to correlate actual physical electrochemical phenomena with the mathematical model per Section 2 and sample readings (data) from the ILI tool.

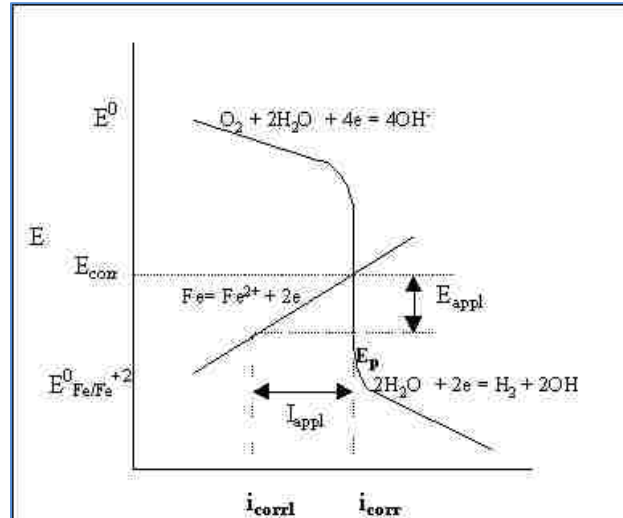


Figure 1.3 – Lazzari and Pedferri – Polarization Diagram of Iron

1.2.2. Corrosion Cell Components. “The electrochemical process consists of four distinct parts: anode, cathode, electrolyte, and metallic path. These four parts constitute what is called the corrosion cell. Electrochemical corrosion occurs only when all four parts of the corrosion cell are present. To understand the operation of a cathodic protection system, it is extremely important to understand these four parts of the electrochemical corrosion cell.

- a. Anode –The anode is the point in a corrosion cell where electricity is passed by chemical means from the surface of the metal to the electrolyte. This chemical reaction is an oxidation reaction, which is characterized by the metal losing an electron and combining with another element, usually oxygen. In the case of steel, the resulting material is iron oxide (rust).
- b. Cathode – This is the location where protection occurs. The cathode is the point in a corrosion cell where electricity is passed by chemical means from the electrolyte to

- the surface of the metal. This chemical reaction is a reduction reaction, which is characterized by the metal accepting electrons to the electrolyte.
- c. Electrolyte – The electrolyte is any material (soil or liquid) in contact with both the anode and the cathode that will allow ions to migrate. The electrolyte is the part of a corrosion cell which allows oxidation and reduction reactions to occur. The electrolyte includes the source of elements or atoms that are required for ion transfer to and from the metal electrodes (anode and cathode).
 - d. Metallic path – The metallic path completes the circuit and allows the electrons to flow. The metallic path is any metal that contacts both the anode and the cathode and allows electrons to flow. This electron flow must be present for electrochemical corrosion to occur. In the case of a tank or pipeline, this can be the tank or pipe itself, or it can be a metallic bond to different metallic structure.”² CP is the manipulation of the corrosion cell components through the control or redirection of current flow as indicated by the arrows (Figure 1.4 below).

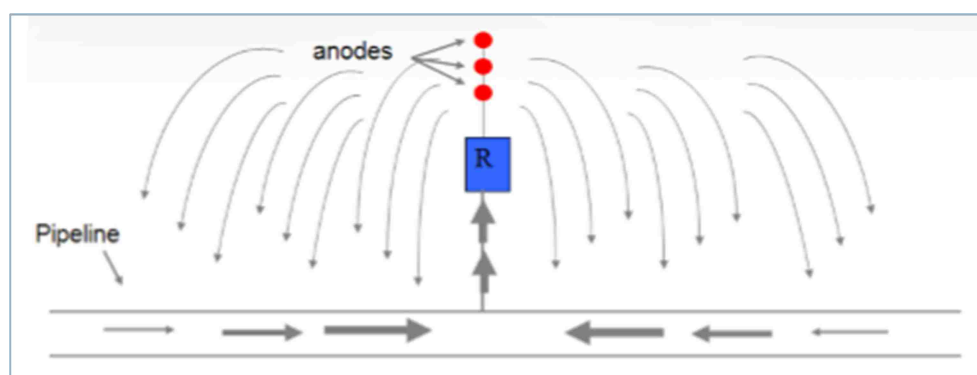


Figure 1.4 – Diagram of CP with R = Rectifier, and Current Flow⁶

⁶ Janda, D.; Williams, D. (2014). “Developing a Standardized Process for Cathodic Protection Current Measurement on In-Service Pipelines – Process and Procedures for a New Technology.” NACE & Baker Hughes: Houston, TX.

The circuit behavior conceptualization is further illustrated in Figure 1.7 in the following section. The Figures 1.1 through 1.6 will help to analyze what is happening in regards to Ohm's Law and possibly with Kirchhoff's theory for summing the contributing electric (or electrochemical) effects across the circuit (corrosion cell). Since a pipeline can be very long, Kirchhoff's methods must consider some integration aspects and boundary conditions. These concepts will be expanded on with additional supporting schematics (see Figure 2.6 and Figure 2.7) as the methodology for solving the engineering problem is outlined in Section 2, since Kirchhoff's alone is not sufficient for solving the problem and Laplacian physics combined with attenuation must be utilized. However, proofs and theories reach beyond this study's objective, which will become clearer in Section 2.

1.2.3. Cathodic Protection Background. This section discusses aspects of CP with respect to its historical use, general design, its relationships to attenuation and calcareous deposits.

1.2.3.1 Brief history of CP. Cathodic protection has been employed as a corrosion control technique for metallic structures, mainly steel enforced masonry, since approximately the 1840's by using zinc alloys as sacrificial anodes. "Since at least the 1930's, CP has been employed as a tool to protect submerged pipelines (below ground or in water) from corrosion, in conjunction with coatings. Over the years, industry has developed techniques to guide the use of CP in practice and design, including recommendations on the use and measurement of CP effectiveness per NACE document SP-0169 and later regulatory standard requirements. One of the main developments was the recognition of the need to establish "criteria" by which the effectiveness of the

application of CP can be judged. Because measuring potential of the steel pipe at a given point was relatively easy, but measuring the current density is much harder; all of the criteria were built around potential measurement.”³

1.2.3.2 Cathodic protection -general design and use. Impressed Current Cathodic Protection (CP), in this case, is used to force the electrons in the redox Equation to the left, recall Equation (1.1) resulting in Equation (1.5), thus slowing external corrosion to reduce to a negligible rate. This is done by inducing low amperage of current flow to the pipeline as defined in the corrosion cell components (corrosion cell circuit) as seen in Figure 1.4 and Figure 1.7.

The power source of the CP is from a rectifier located alongside of the pipeline that supplies amperage to maintain a constant potential across two electric terminals (anode –soil electrolyte and cathode -pipe). Through years of empirical and lab research, it has been discovered that the required negative shift in cathode potential for effective prevention of corrosion is approximately -100mV (millivolts).⁷ Although this is not indicative of achieving E_{eq} ; rather, the anodic reaction rate becomes so low that external corrosion becomes negligible.⁷ It is not necessary to achieve the value of E_{eq} , however, it is more important to get close enough to the value so corrosion is rendered trivial. In industry the shift or potential drop has several commonly used terms: a) polarization, b) potential shift, or c) over potential, all of which have the same meaning. On a pipeline with effective CP, the current density and the potential over time will be controlled by the calcareous deposit (Figure 1.2, and Figure 1.5 – Figure 1.7).

⁷ Mateer, M; Pikas, Joe, Williams, D.; (2017, April 03). *General agreed concept, throughout industry.* Discussions with industry SMEs from Shell, Technical Toolboxes, and BHI.

There are many sources that may lead to the failure of below ground steel pipelines that could result in consequential impacts to the environment, safety, and economics etc. CP is specifically designed to inhibit external corrosion of these buried structures. The first line of defense to external corrosion is the coating of metallic structures via epoxies (i.e. FBEs – fusion bonded epoxy), coal tar enamel (CTE), tape coat, or extruded polyethylene to name several examples. Coatings can fail, disbond (coating detachment from metal), delaminate, form holidays (type of coating defect of disbondment), or shield (allow water and oxygen to contact the pipe, but prevent CP current from doing so). “Native (bare) steel is defined to have an approximately -500mV rest potential. The impressed current must have a polarization shift of -100mV from the native state (also known as the corrosion potential in soil) which puts the desired target range of -600mV to -850mV polarized potential versus a saturated copper to copper sulfate electrode Cu/CuSO₄. This potential target range is mandated to be maintained by standards and regulations.”⁸ This negative “potential shift from E_{corr} (overvoltage or $\Delta E_L = E_L - E_{corr}$) was developed based on empirical testing and theoretical principles. Because current density measurements were so difficult, no CP protection criterion was ever developed around current density.”⁷

Corrosion is the deterioration and degradation of a material as described in Sections 1.2.1 through 1.2.1.2 above which eventually causes structural failure of the metal (metal loss). There are several types of corrosion for metal but it can only occur through a “corrosion cell” which is a complete circuit as conceptually re-depicted in Figure 1.7 (below).⁷ The electrochemical process can be controlled such that the ions are

⁸ Williams, D. (2017, March 31). Background on Corrosion, CP, CPCM Data Analysis Telephone interview. Discussions with David Williams (CP Specialist & NACE CP4 Certified at BHI).

redirected to exposed areas where ion reduction occurs at the metal pipe surface. The concentration of current is the greatest at the supply (rectifier) as seen in the figure below. “When the entire pipeline surface is provided with sufficient current density to react with all the oxygen diffusing to the surface, corrosion rates will drop to an extremely low value and a calcareous deposit will form.”⁷

1.2.3.3 CP and attenuation. Potential attenuation with distance from the rectifier drain point is based on empirical behaviors of ohmic drop of the metal pipeline of which current propagates through over distance. Attenuation will vary in real world applications as steel material alloys are not perfectly uniform, temperatures fluctuate, geometry can vary, and as the soil conditions change etc. over the distance that a pipeline traverses. Attenuation is an important phenomenon in physics, “attenuation is the gradual loss of the intensity of any kind of flux, through a medium.”⁹ In this case the flux is the current density of a pipeline, where the medium is the complete circuit as defined in Section 1.2.2 per the length of the pipe.

1.2.3.4 CP and calcareous deposit relationship. “The cathodic reaction at the pipe metal/soil interface will often cause a gradual change in the pipe potential by polarization. This occurs by the formation of resistive calcium salts which are plated out from the ground and can reduce the current demand on a poorly coated surface by 60 to 80 percent.”¹⁰ On a real pipeline system with CP, calcareous deposit is typically comprised of mineral combinations of calcium carbonate (CaCO_3) and magnesium hydroxide ($\text{Mg}(\text{OH})_2$) that become deposited (precipitated) as conveyed in (Figure 1.4,

⁹ Nicholson, J.P. (2011), “Pipeline Integrity, Pipeline Corrosion Control.” *World of Pipelines*, Cathodic Technology Ltd., CAN

¹⁰ Morgan, J. (1987); “Cathodic Protection” (2nd Edition). NACE, Houston TX, Chapter 2 and APPENDIX D.

Figure 1.7, and Figure 2.2) onto a cathodically protected surface.⁷ “The result is an increase in the pH at the soil pipeline interface, and the formation of hydrogen on the surface of the pipeline; a situation commonly referred to as polarization.”⁹ Steel’s corrosion rate increases when the pH is below 4. Steel dissolves at pH of 3. The pH adjacent to the surface is dependent upon the soil condition (or electrolyte).¹¹

These calcareous minerals are insoluble in a high pH and build up deposits (collecting in masses) over time on the coating. These mineral deposits eventually increase the coating resistance, but also slow the diffusion of O₂ to the pipe surface. Since current depends on the potential shift and the coating resistivity through Ohm’s Law, as the coating resistance increases then current will decrease. The following photographs (Figure 1.5 and Figure 1.6) are examples of an unearthened pipe that shows how the CP helped create a calcareous deposit over time at the shrink sleeve and coating interface on the exterior of a pipeline.



Figure 1.5 – Part 1, Calcareous Deposit Example –Shrink Sleeve & Coating Interface

¹¹ Mateer, M.; (2017, April 3rd- 4th). *Background on Corrosion and CP, CPCM Data Analysis Approach* [Telephone interview #2]. Discussions with Mark Mateer, Principal Asset Integrity Engineer.

“A large calcareous mass has been deposited by the pipeline’s cathodic protection system over a defect in the heat-shrink sleeve used to coat a field joint girth weld.”¹²



Figure 1.6 – Part 2, Calcareous Deposit Example –Shrink Sleeve & Coating Interface¹²

“The rough appearing surface to the left of the corrosion product buildup is the heat shrink sleeve adhesive that remained on the pipe after the sleeve was removed. Note that the pipe was not corroded beneath the calcareous deposit, but was corroded beneath the disbonded heat-shrink sleeve.”¹²

The ultimate goal is to achieve effective, consistent CP and the sure sign of a protected line is resultant calcareous deposit. The calcareous deposit mineral substance adhered to the surface of the coating and or the pipe, “where a protective calcareous deposit can only be formed if the over potential (polarization) is sufficient to prevent corrosion.” When a pipeline becomes polarized (Figure 1.3 and Figure 1.7), the current

¹² Bash, R. (2011), “Observations From 56 Years Of Pipeline Corrosion Damage Excavations” *Pipeline & Gas Journal*, Volume 238, No.3; <https://pgjonline.com>

stabilizes and the OH^- generated by the current raises the pH at the surface of the pipe and over time a calcareous deposit will build up. The calcareous deposit limits oxygen diffusion per Equation (1.6) lowering the current needed for protection.

“CP causes the surface to polarize and requires less current to achieve a lower potential. This can be due to calcareous deposit, but can be caused by other effects as well. For CP on pipelines, this is almost always due to calcareous deposit formation.”¹¹
 The use of a coating will reduce the overall current density required for protection.”^{7 & 8}
 The resistances within the Figure 1.7 of R_1 , R_2 , R_3 , and R_o are fixed, but R_4 varies with the length and geometry of the pipe in accordance to Equation (2.16).

R_o is the constant resistance of the coating. Figure 1.7 assumes an infinitely long pipe, where the over-potential varies by $\Delta E_x = \Delta E_o e^{-ax}$, such that ΔE_x represents the polarization at point x and ΔE_o is over-potential at the drain point; however of greater concern with respect to the problem statement, the current expression is most important and varies as $\Delta I_x = \Delta I_o e^{-ax}$.

These variables and Equations are introduced here, but are important as they will be discussed in more detail later in the Section 2.3 for CP ANALYSIS, regarding cathodic protection. Currents and potentials must be as constant as possible within a CP system. There are many factors that impact CP, changing the current or potentials through the interruption of the current causing increases in corrosion rates, or areas where certain features “leak” current, or other systems’ stray currents interfere with the CP system. It is important to engineer or balance these circuits to reduce the interference effects on other CP systems, since many things can impact, alter or influence current.

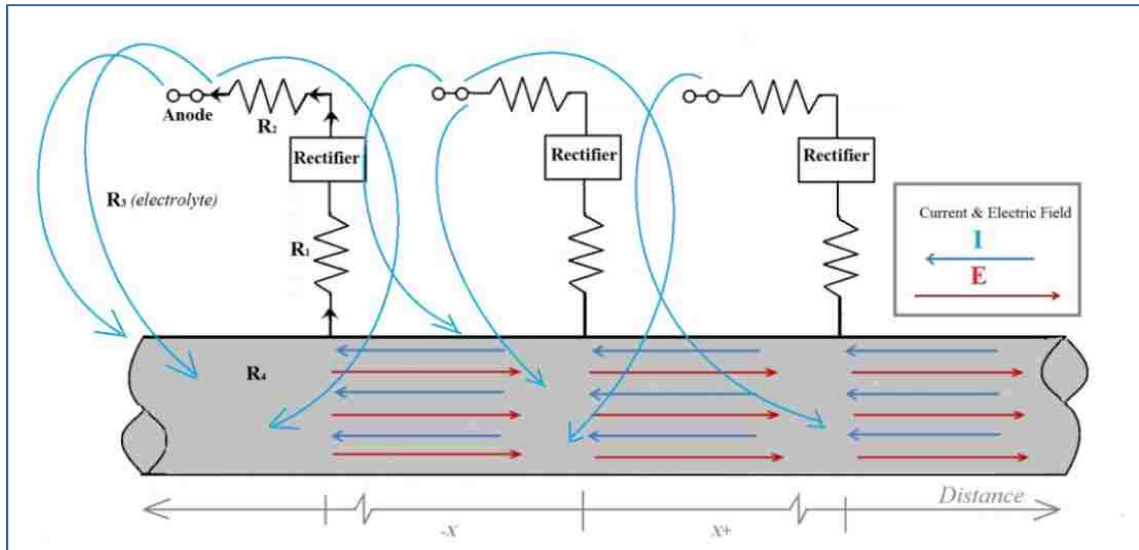


Figure 1.7 – Image Redrawn from “Cathodic Protection” –Lazzari & Pediferri¹

This study will show how measuring CP’s effectiveness is possible through inline inspection devices through examination of the entire circuit and related potentials. This study will address the capabilities of the tool to successfully measure current density and therefore voltage.

1.2.4. Regulatory Requirements for CP. CP of buried pipelines is important and is only one of many specific requirements by the regulations for oil and gas under Title 49 CFR (Code of Federal Regulations) Parts 192 and 195 and enforced by PHMSA (Pipeline Hazardous Materials and Safety Administration) to prevent and mitigate corrosion and help maintain integrity of the pipeline system.

There are many standards that apply to fulfil these regulations such as NACE, API, ANSI/ASME etc. for designing CP to help prolong asset life, maintain safety, and protect surroundings against possible in-service releases (pipeline failure) caused by external corrosion and therefore the need for preventing and mitigating consequential damages. The idea is to proactively mitigate possible failure from corrosion by

maintaining consistent and effective CP systems. Close Interval Surveys (CIS) – also known as pipe-to-soil and potential gradient surveys – are one of several methods for assessing effectiveness of cathodic protection (CP) systems used on buried pipelines.¹³ The CP ILI tool helps to satisfy the CIS requirement for assessing CP as well as many other benefits documented in the following Section 1.2.5.

1.2.5. Use of ILI Tool for CP Measurement. In industry the measurement or inspection and evaluation of CP and its effectiveness is not conducted with ILI tools for horizontal pipelines. The CP ILI tool is one of a kind for buried pipelines' to fulfill this measurement effort in place of CIS and other benefits, as explained previously as well as many other benefits summarized herein.

Test stations are used to measure IR drop and are digital; however, the CIS methods are still very manual. The CP ILI tool helps to automate the majority if not all of the CIS and some other related CP system monitoring potentials from inside of the pipe. The CP ILI tool is designed to support integrity of a pipeline specifically with respect to external corrosion prevention and mitigation through a more proactive approach by being able to monitor CP systems remotely from inside of the pipeline instead of manually from outside of the pipeline. The CP ILI tool is made to measure current density in the pipe by how much current is entering the pipe at every point to directly be able to read an IR drop of the pipe. With applications of Ohm's Law in combination with Kirchhoff's circuit theory and attenuation, which is covered in Section 2, various potentials and or parameters can be determined and or considered. In

¹³ Pipeline Hazardous Material and Safety Administration (PHMSA) "Fact Sheet: Close Interval Survey", <http://primis.phmsa.dot.gov/comm/FactSheets/FSCloseInternalSurvey.htm>, 2017.

support of integrity management, the overall usefulness and benefits of the CP ILI tool to industry presented by BHI and SMEs are the following:

- Locate and quantify ALL current sources
- Define current source boundaries – Identify midpoints
- Locate and quantify shorts/bonds
- Define areas outside of any current influence
- Define coating quality based on ACTUAL current densities
- Access to 100% of a piggable pipeline regardless of the ROW (right-of-way, easement) location, terrain, or condition
- Cost effective – people are scarce and expensive. Time to complete a full survey is reduced from weeks to days or hours.
- Better utilization of resources - personnel have more time to focus on solving problems by spending less time gathering data
- Reduced HS&E exposure to personnel in the field
- Up to three data sets per inspection - CP Current Inertial mapping Caliper
- Seamless integration with other ILI data and GIS Systems
- Recordable, accurate, and repeatable
- No landowner or ROW access issues
- CP System left on – no interrupters to set and keep synchronized
- Measures most stable leg of CP circuit – outside influences are minimized
- Locate areas prone to corrosion before damage occurs.¹⁴

¹⁴ Janda, D.; Williams, D. (2010). "Inline Cathodic Protection Monitoring." World of Pipelines & Baker Hughes: Houston, TX

1.3. INTRODUCTION TO THE CP ILI TOOL

CP current measurement using an in-line inspection (ILI) tool is a proven technology. The general principle of the tool is related to some design aspects of the vertical downhole exploration technology methods (i.e., The Atlas VertilogTM) for CP measurement then applied to horizontal submerged pipelines. The difference in the design for horizontal pipelines using a “smart pig” is that the tool travels down (traverses) the pipeline which presents some complications compared to the vertical downhole tool.

The CP ILI tool gathers current density data of horizontal pipelines and voltage data using the conductive contact to the surface of the interior pipe wall to find direction and magnitude of CP and other current changes or stray current on the pipe (Figure 1.8). The sensors of the tool are separated by a distance of approximately 1.38 meters (~6 feet) to give the IR at that distance on the pipe. The orientations of the sensors are polar in design, with positive on the back and negative on the front of the tool. The idea of the polar concept helps with determining the direction of current flow impressed on the pipe with respect to any distance from the rectifiers.

Later in this paper some suggestions for future research for modification of the sensors and area of coverage will be presented among some other research ideas after navigating through the engineering methodologies and data findings with respect to the research objective of this thesis stated in Section 1.1.

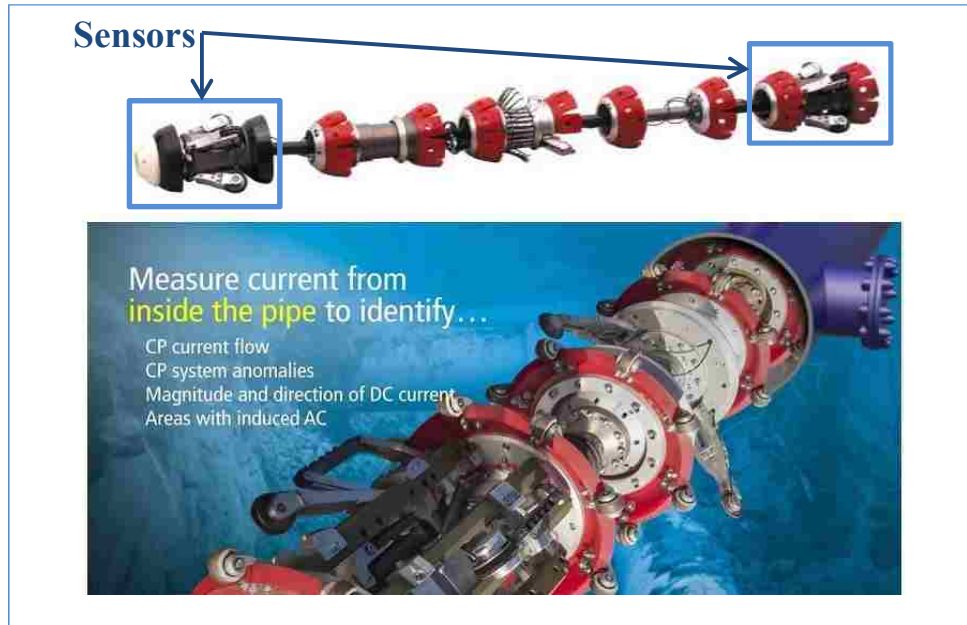


Figure 1.8 – Baker Hughes Public Video www.BakerHughes.com¹⁴

The CP ILI is designed to make IR drop readings, which are converted into a current density through Ohm's law and upon dividing it by a distance to get (Amps/m²) or Amps/ft²). This is an area density term and can be included in the following Ohm's and Kirchhoff's methods as in Section 2. Regulations require that a voltage be measured to the shifted -100mV (recall desired range in Section 1.2.3). Since regulators enforce measurement by voltage rather than by current, this paper will demonstrate the physics to show that it is possible to measure and convert the appropriate terms and variables via applications of Ohm's Law, attenuation, and Kirchhoff's theory. More specifically, the use of electrochemistry combined with the aforementioned laws conveys that current density can be converted into a potential (voltage) for certain terms and variables. These methods will be applied to the CP ILI device's sample data of a pipeline (data from BHI).

The CP ILI experiences some noise and vibrations in liquids (i.e., gasoline) and fewer vibrations in crude oil pipelines. There some are averaging techniques used in the

analysis of the data samples taken by the tool to help separate good data from noise. Reduced vibration helps to get better readings for determining the current density changes (losses or increase of current) of a CP system due to some expected features as well as other less desired issues. Some of the undesirable irregularities are: coating problems, holidays, actual corrosion, stray current, shorts, bonds, proximity to other pipelines etc. Irregularities in the current can be detected and then corrected to prevent or mitigate corrosion or other issues that could impact the life, health, and safety of the pipeline. When the ILI tool's sensors make contact with the internal pipeline surface in Figure 1.9, then the circuit in the corrosion cell is complete, as illustrated previously in Figure 1.7.

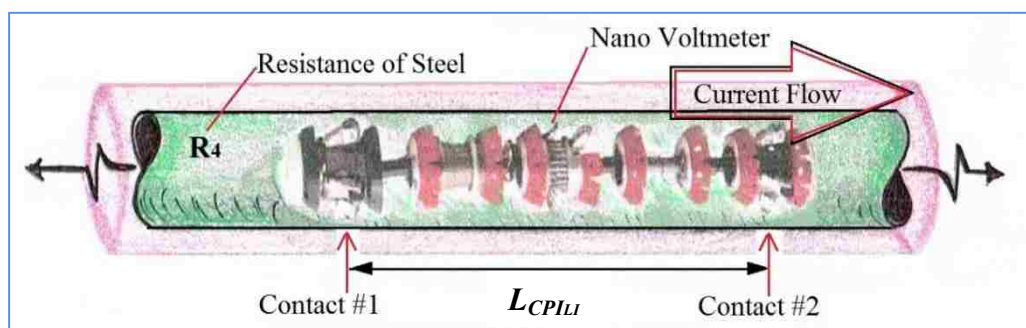


Figure 1.9 – CP ILI Within the Pipe Conceptualization

Noise becomes more stabilized in certain liquids pipelines because of the viscous fluid nature to help with dampening of vibrations etc. This study touches on those issues that need to be fine-tuned, but is not part of the scope. The present need is for identifying the appropriate physics to support the problem statement with respect to the ability of the tool to get a pertinent signal in general that is measureable for pipe-to-soil potential. Future suggestions shall be made based on the findings from Section 2 and

then later discussed in Sections 3 and 4 concerning other potential inhibitions or troubleshooting methods as they become apparent, but again those concepts reach beyond the scope of this thesis.

By CP design and close interval survey (CIS) requirements, operators typically use 4-wire IR drop (voltage drop) test points along a pipeline to measure the voltage and calculate the current vector per the following:

- a. Measuring current returning to rectifier on either side of the active rectifiers,
- b. Measuring current vector of random lengths along the pipeline,
- c. At points based on specific criteria (problem areas, regulated, and corrosion susceptible areas).

Voltage (IR) drop test stations' contact wires are tack welded along the pipeline separated by a distance of resistance per unit length, from 15.24m (*50ft*) to 30.48m (*100ft*), which is dependent upon the pipe geometry (OD, wall thickness),¹⁵ *see* also Section 2. Pipe resistance is also referenced in industry standard pipe tables, which are included in the appendix. The resistance can be calculated by applying specific current across a certain distance then using Ohm's law to find the voltage drop, which is a similar process to test station calibration. This establishes the current's known parameters per pipeline attributes and a starting point in order to build CP ILI "in-line runs" baseline comparison data. Anywhere the coating is compromised or the pipeline is exposed, the current will increase. Through Ohm's law, the current will decrease as resistance increases; therefore, an object in the path of impressed current may reduce the current. Also, a lower over potential could cause a lower current.

¹⁵ Janda, D.; Williams, D. (2014). "Developing a Standardized Process for Cathodic Protection Current Measurement on In-Service Pipelines – Process and Procedures for a New Technology." NACE & Baker Hughes: Houston, TX

Preventing corrosion is the first objective and to do this proactively through the use of CP and continuously monitoring its system by automated or robotic CIS via ILI may help alleviate some challenges, inefficiencies, and dangers of performing manual surveys and site tests in difficult terrain etc. Although each pipeline is different, it could eventually lead to some standardization of processes and how data can be assessed. Surveys would take far less time and manpower. The use of the tool itself may help prevent some field safety issues, which supports P&M (preventive and mitigation) measures, which additionally satisfy needs for monitoring of CP systems by regulations.

These previous sections provide background, definitions, and lead to the technical supporting publications and then the engineering methods within Section 2 that explores the ability of the tool to gather pipe-to-soil IR drop (current and resistance) measurement data of a steel pipeline in order to apply some physical applications of Ohm's law, Kirchhoff's theory, combined with attenuation.

2. ENGINEERING ANALYSIS & METHODOLOGY

This section outlines the methodologies for analysis on available physics for an impressed current CP system.¹ The problem approach is outlined directly below which considers a closer look at CP assessment through CP ILI data analysis through a mathematical model built from Equations and methods in this section. Collaborative assessments with industry experts (See Acknowledgements) to confirm the tool's ability to gather current density readings per the methodologies of this section that can be converted to pipe-to-soil potential measurement will be discussed in Sections 3 and 4.

2.1. PROBLEM APPROACH

- a. Identify and discuss assumptions;
- b. Identify and discuss application of CP on a pipeline (realistic scenario);
- c. Identify how the CP ILI finds current density via sample data;
- d. Show the applied physics for attenuation and relationship to part c. above;¹
- e. Investigate applicable circuit behavior via a mathematical model;
- f. Visually convey and present data findings to support the above listed items.
- g. Methodology Goal - To be able match results from the CP ILI tool sample data through the mathematical model via the following parameters:
 - 1) For the first group of plots the over potential ($\Psi_L = E_L - E_{\text{corr}}$) at the midpoint (drain point) will be held constant at a -100mV shift and then vary the coating resistivity.

- 2) For the next group of plots, the coating resistivity shall be held constant at the commonly found 450,000 Ωm and then the over potential Ψ_L will be varied.

2.2. ASSUMPTIONS

To establish physical relationships for this study, the following will be assumed. As noted by industry experts, “A pipeline’s linear resistance is essentially fixed. Unless a pipeline is modified or changed, the resistance across a given section of pipe does not change with time.”¹⁶

- a. One- dimensional steady state conditions (for energy transfer)
- b. Uniform metal:
 - i. API 5L, Grade X42 (alloy content) ,
 - ii. uniform smooth surface, 12” OD (NPS) = 12.75”OD & standard 0.5” w.t.,
 - iii. uniform thermal conductivity k (carbon steel₁₀₁₀ $\sim 1.43 \cdot 10^{-7} \Omega\text{m}^{-1}$),

$$k = \frac{1}{\rho} = \text{electrical conductivity coefficient } \Omega\text{m}^{-1},$$
 - iv. Low carbon steel only as in Section 1.2.1.2.¹⁶;
- c. 80% coating efficiency (η) for FBE (fusion bonded epoxy);
- d. distance between rectifiers is 7260 m = $\sim 25,000$ ft;
- e. constant ambient pressures and temperatures;
- f. isothermal (constant temperatures with no other transients or losses):
 - i. Surfaces
 - ii. Surroundings

¹⁶ Pioneer Pipe (2014). “Standards and Specifications”, 5th Edition 11. Houston, TX.

iii. Internal Medium (fluid flows)

- g. For Section 2.5 assume the CP ILI tool resistance R_5 considers complete contact for the entire length of the tool at 1.83 m (~6ft) with no other losses (ideal);
- h. Neglect friction due to tool contact with internal pipe surface roughness;

Numerous effects impact pipeline systems creating inconsistencies and transients in system analyses due to irregularities (anomalies), variations in terrain (soil pH conditions), fittings, and components. No two pipeline systems are identical. Current and voltage measurements must be established and tested to illustrate trends for a system of concern. The above listed assumptions are subject to real world variances per operating conditions, but this study will examine and address the phenomena in a simplified fashion (ideal) with constant variables to illustrate what is happening with the physics concerning the pipe-to-soil potential. These other listed assumptions are not limited to the following:

- i. Soil conditions: uniform constant pH (electrolyte), moisture and temperature for the calculations. Uniform/constant soil electrolyte composition range is from 1 to 6 mA/ft² (see APPENDIX for more values, but in general 10 to 60 mA/m²).
- j. Data is for a ~20-year old pipeline with FBE (fusion bonded epoxy) coating.
- k. Assume pipe and omission of appurtenances that impact bulk metal content, which change pipe IR such as: valves, equipment, meters, or sleeves (shorted dielectric filled sleeves or normal weld sleeves).
- l. Excludes stray current/interference from other systems or overhead wires.
- m. Pipeline has attenuation, derived from Lazzari and Pedferri's (L&P) methods: ¹
 - i. Attenuation is gradual loss of intensity of energy flux through a medium.

- ii. Boundary conditions are applied via Laplacian to get appropriate resistances per boundary conditions over designated pipe lengths.
- n. Theoretical approach for analyzing the CP ILI data:
 - i. Conductance leakage to earth is uniform for the total length of line
 - ii. Current loss (drain) from pipeline is at a point and discharges to the ground a distance away so the anode cannot be detected at the pipeline (see Figure 1.4, Figure 1.7, and Figure 2.6).
 - iii. Uniform shape, geometry of pipe implies uniform characteristic resistance.

2.3. CP ANALYSIS

This section relates to the background of CP defined in Section 1.2.3. This section applies analytical methods from Lazzari and Pedferri¹ with respect to attenuation. Once the current is induced, the current density will be the highest at the “drain point” (as illustrated in Figure 2.1), and then the current density will gradually decline while the horizontal distance grows in either direction on the pipeline away from the drain.⁷ “This phenomenon is due to the constant pipe potential and again as the circuit resistance increases (pipe resistance increases with length) over a distance travelling away from the drain point.”¹¹ Both potential and current density are largest at the drain point. The following Figure 2.1 can be likened to the conceptual circuit conveyed previously in Figures 1.7 and 2.2, but without the current flow arrows, which is later clarified in Figure 2.6 and Figure 2.7 which includes the CP ILI tool’s resistance.

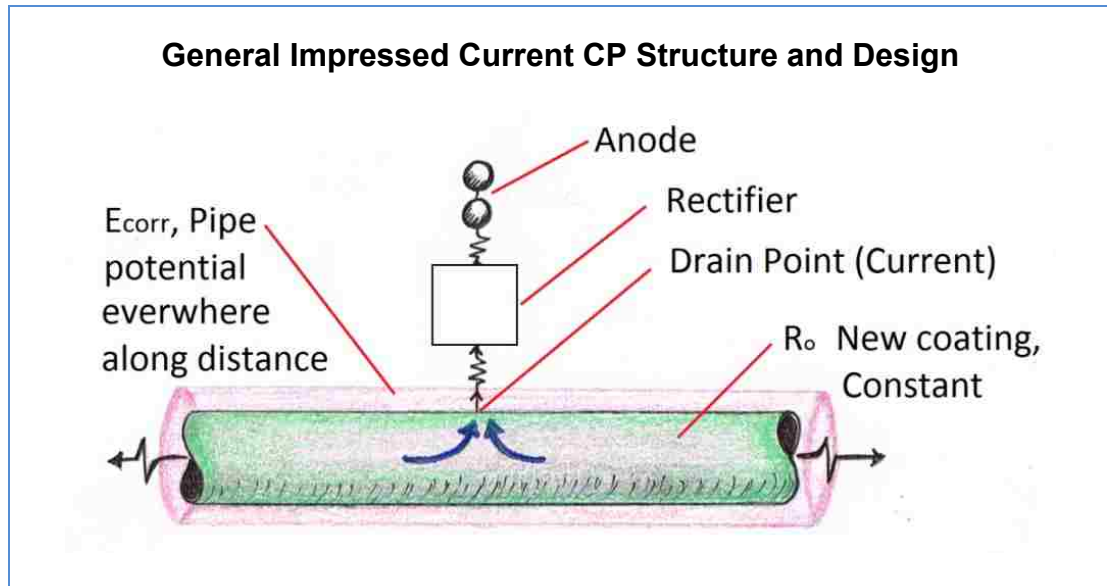


Figure 2.1 – Pipeline Schematic for Analysis¹

The boundary conditions for applying the impressed current are based on four domains, which can be further related to attenuation later in Section 2.4 per the conceptual diagrams Figure 2.1 through Figure 2.3.

For Figure 2.2 and 2.3, “Consider a pipeline which is not in equipotential because of an ohmic drop in the metal. Current and potential distributions are obtained by solving the field Equation on the basis of the following boundary conditions in the pipeline:

$$\nabla^2 E_m = 0 \quad \text{Laplace} \quad (\text{domain 1})$$

$$E_c = E_m - \eta_c; \quad \& \quad i_c = f(\eta_c) \quad (\text{domain 2})$$

$$E_{\text{electrolyte}} = \text{constant} \quad (\text{domain 3})$$

$$E_{\text{anode}} \quad \& \quad I_{\text{anode}} = \text{constant} \quad (\text{domain 4})$$

E_m = potential of the metal \neq constant; E_c = pipeline potential, which eventually includes both the polarization η_c and ohmic drop in the metal (ΔE_m); and i_c is cathodic current density on pipeline surface.”¹

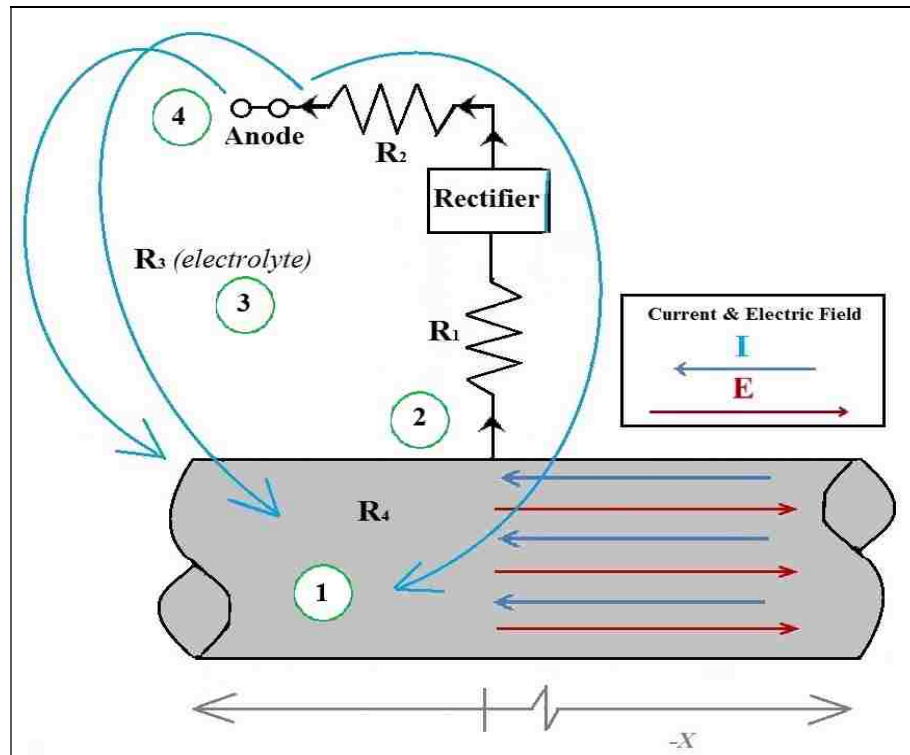


Figure 2.2 – Pipeline Schematic, Redrawn Relating to Figure 2.1 for Analysis¹

The potential and current attenuation concepts are drawn in the graphs of Figure 2.3 and later described in Equation sets (2.1) through (2.9). Notice by Ohm's Law, that the relationships can be established in general for the current density and the potential, hence the similarity in the shape of the graphs, where both the current density ΔI_o as and the over-potential ΔE_o (Figures 2.1 through 2.3) will be greatest at the drain point (rectifier source). These concepts, in addition to the boundary conditions, lead to the attenuation methods of the next section.

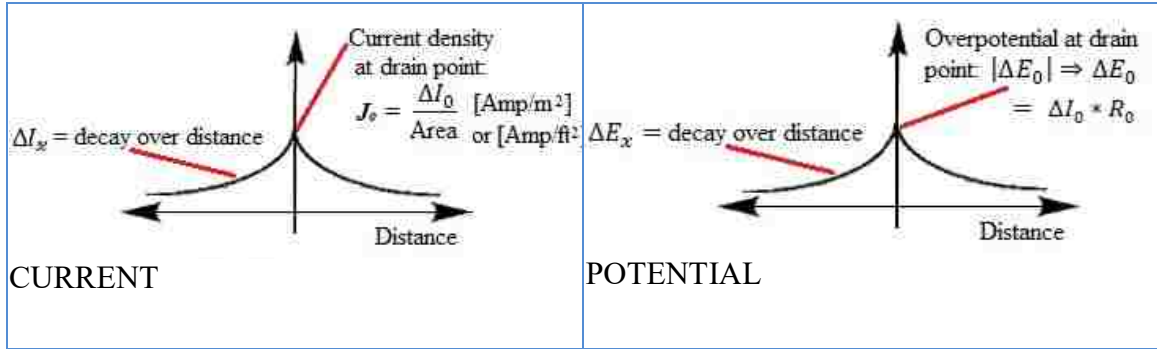


Figure 2.3 – Attenuation Trends for Current and Potential

2.4. ATTENUATION of CURRENT & POTENTIAL

For the Equations of this section, all of the symbols for ‘ E ’, ‘ Ψ ’ and Φ , represent potential. Any annotation ‘ R ’ is representative of resistance and the subscript denotes particular elements from the system’s resistance. The letter ‘ I ’ indicates current. For the following physics, $\Delta I'_0$ and $E I'_0$ denote the potential shift and current shift by a change of $(2L-x)$, which is the two drainage points of the pipeline length L (as in Figure 2.2 and Figure 2.3), of which L is the half distance between the rectifiers and finally x is a remote distance.¹⁰ The physics of the problem are as follows in relation primarily to attenuation derivations from the Lazzari and Pedeferrri approach, Chapter 4¹ and historic Morgan chapter 2 and Appendix D (Attenuation Constants).¹ The boundary condition, from Figure 2.1, helps establish the Ohm’s Law relationship with respect to the geometry of the CP system. “The Laplace Equation (in Figure 2.1) refers to an ohmic conductor; therefore its solution is Ohm’s law at a distance x from the drainage point.”¹

The shift of $\Delta I'_0$ and $E I'_0$ propagation by hyperbolic cosine is defined mathematically in Equations (2.5) and (2.9) and with respect to attenuation.¹⁰

$$\Delta E_x = \Psi_x = \Phi = \Delta I_x * R_o, \text{ through Ohm's Law, where} \quad (2.1)$$

Equation (2.1) can be written as follows:¹

$$\Rightarrow \Delta E_x = \Delta I_x * R_o \cosh(a_{att} * (L - x))$$

$$\Rightarrow \Delta E_x = \Delta E_L \cosh(a_{att} * (L - x))$$

Or as a final form, from Equation (2.1) above

$$\Rightarrow \Delta E_x = \Psi_x = \Psi_L \cosh(a_{att} * (L - x)) \quad (2.2)$$

Where,

$\Psi_L = E_L = E_o$ is the over potential (drain point) and

$$\Psi_L = (E_L - E_{corr}) = -0.1 \text{ Volts, electrode shift}$$

The E_L value is typically the Cu/CuSO₄ potential and is approximately -0.65 to -0.85V for the electrode to help get the appropriate over potential Ψ_L shift of -0.1V as required by regulations.

Within the model for the CP ILI data to get outputs for Section 3, the coating resistance is fashioned from Lazzari and Pedeferr¹ in addition to various similar references, industry knowledge and experience to input relevant data such as for the coating efficiency η and coating R_o resistance.

$$R_o = \rho * \left(\frac{\eta * d}{Area} \right) \quad (2.3)$$

Where d = the coating thickness.

Area includes the thickness of the pipe, $Area = \pi * (r_2^2 - r_1^2)$ and $r = radius$ (outer denoted by subscript 2 and inner by subscript 1 respectively).

For the coating efficiency the following Equation is used.²¹ This research assumes 80% efficiency in the model for conservative measure.

$$(2.4)$$

$$\eta = \left(1 - \frac{I_{coated}}{I_{bare}}\right) * 100\% \quad (2.5)$$

$$\Delta E_x = \Delta E'_0 e^{\alpha_{att}(2L-x)} + \Delta E'_0 e^{-\alpha_{att}x}$$

$$\Rightarrow \cosh(u) = \frac{e^u + e^{-u}}{2}, \text{ from the identity, hence the } (2.6)$$

$$\Rightarrow \Delta E_x = \psi_x = \Delta E_L \cosh(\alpha_{att}(L-x)), \quad (2.6)$$

Where,

$\Delta E_L =$ over potential at the drain point;

$L =$ the distance to the midpoint;

$x =$ distance from the drain point; and

$$\alpha_{att} = \sqrt{\frac{R_4}{R_t}} = \text{attenuation constant.}$$

The first R_4 immediately following was used in the model as per Lazzari

and Pedferri.¹ (2.7)

$$R_4 = \rho * \frac{L}{A} = \frac{L}{k * \pi * (r_2^2 - r_1^2)} = \text{Longitudinal resistance of pipe;}$$

$$\text{recall } \rho = \frac{1}{k} = \text{resistivity } \Omega\text{m}, \quad k = \text{conductivity } \Omega\text{m}^{-1}$$

$$\text{By Laplace, for cylindrical w. t.,} \quad R_4 = \frac{\ln\left(\frac{r_2}{r_1}\right)}{2\pi k L} = \rho \frac{\ln\left(\frac{r_2}{r_1}\right)}{2\pi L}$$

$$R_k = \sqrt{R_4 R_t} = \text{Characteristic resistance of the steel pipe;}$$

$$R_t = \frac{R_o}{\pi D} = \text{transversal resistance based on coating resistance.}^1$$

From Ohm's Law the following relationship is established.

(2.8)

$$\Delta I_x = \frac{\Delta E_x}{R_o} = \frac{\Psi_x}{R_o}$$

Where R_o = coating resistance, see also Equations (2.4) and (2.3), refer the Appendix for coating efficiency ²¹ and related potential.

$$\Delta I_x = \Delta I'_0 e^{-\alpha_{att} x} + \Delta I'_0 e^{\alpha_{att}(2L-x)} \quad (2.9)$$

$$\cosh(u) = \frac{e^u + e^{-u}}{2}$$

Therefore the current density Equation below will be used to model the results of the CP ILI data. (2.10)

$$\Rightarrow \Delta I_x = \frac{\Delta E_x}{R_o} \cosh(\alpha_{att} (L - x)) = \frac{\Psi_L}{R_o} \cosh(\alpha_{att} (L - x))$$

$$\Psi_L = E_L - E_{corr}$$

Per Ohm's Law, the following substitution is:

$$\frac{\Delta E_x}{R} \Rightarrow \frac{(E_L - E_{corr})}{\left(\rho \frac{L}{\pi * (r_2^2 - r_1^2)} \right)}$$

After substituting the above into Equation (2.7), then the current can be rewritten in terms of ΔE_x through Ohm's law. That is the desired final calculation, where ΔI_m is provided from the CP ILI tool data from BHI per Figure 3.1 through Figure 3.3. The model is matched the CP ILI data by ΔI_x (predicted) from which the ΔE_x (cathode potential) as seen in Figure 3.4 through Figure 3.28 from the results Section 3.

2.5. ANALYTICAL VIEW PER CP ILI

This section discusses the physics with how the CP ILI tool works from inside of the pipeline. The CP ILI measures current at various places along the pipe by making

internal contact at both ends of the tool (see Figure 2.4). There is some software unique to the tool, so the tool can upload its data and then be converted into a current density $J = \Delta I / \text{Area}$, which is gathered from along the line and will look like Equation (2.11). It is important to make note of the relationships of ΔI_x in Section 2.5 below per Equations (2.8), (2.10), and (2.11) since this is what the CP ILI tool is gathering and what the mathematical model is matching to. The physics of the CP ILI tool will look like the following in addition to the attenuation applications:

$$J = \text{current density} = \frac{\Delta I_x}{\text{Area}} \Rightarrow \Delta I_m \quad (2.11)$$

The tool measures the IR drop of the pipe by $\Delta E = IR$ from Ohm's Law, where in this case from the tool's view, $R_5 =$ resistance of the CP ILI tool. This configuration will show up again per application of Kirchhoff's theory in Section 2.6.2.

$$R_5 = \frac{L_{CPCM}}{k * \text{Area}} = \frac{\rho L_{CPCM}}{\pi * (r_2^2 - r_1^2)} \quad (2.12)$$

$$\Delta E = (E_1 - E_2) = \Delta I_m * \left(\frac{\rho * L}{\pi * (r_2^2 - r_1^2)} \right) \quad (2.13)$$

Therefore by Ohm's Law the result written in the form of current is per the Equation below, where I_m is the current measured at any point on the pipe:

$$\Rightarrow \Delta I_m = \frac{(E_1 - E_2)}{\left(\frac{\rho * L_{CPCM}}{\pi * (r_{OD}^2 - r_{ID}^2)} \right)} \Leftrightarrow \Delta I_x = \frac{\Delta E_x}{R_5} \quad (2.14)$$

To see the Kirchhoff's method considering this element of R_5 , refer to Figure 2.7 and the supporting analysis for details. The CP ILI tool contact with the pipe will look

similar to Figure 2.4 (Parts a. & b), where the tool will sum the points over small distances and store the information and then later it will be downloaded to BHI software and then be converted into a density 'J' from Equation 2.11. In this example below of Figure 2.4 (Parts a. & b), $\Delta I = \Delta I_m$ as from Equation 2.14. Ultimately, the steps in this analysis will lead to the overall potential calculation from the view of the tool yielding ΔEx which is the desired polarization of the cathode.

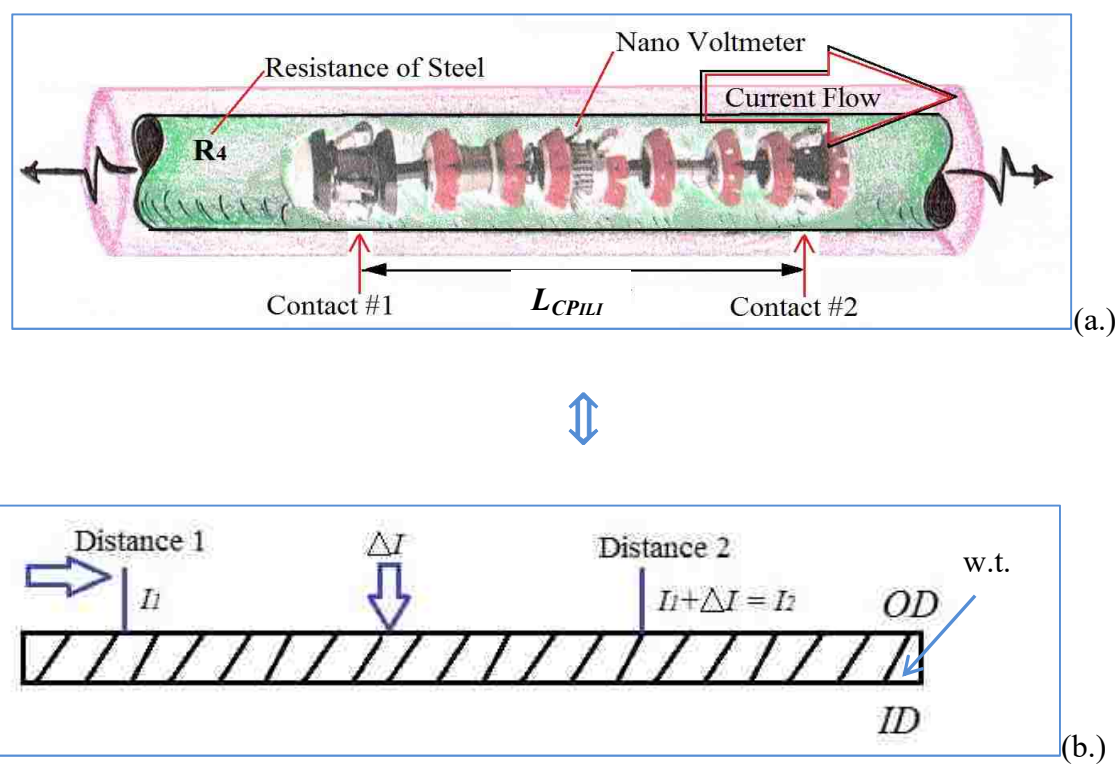


Figure 2.4 – Tool Reading - Sensor Contact Points 1 & 2 (Parts a. & b.)

2.6. KIRCHHOFF'S & OHM'S LAW for CORROSION CELL

Ohm's law combined with Kirchhoff's theory is a common empirical method used to approximate voltage across circuits and current through materials. Ohm's law can help establish a relationship between current and voltage where they are proportional

to each other. The constant of proportionality is I/R , the current divided by the resistance of the material. The arrows (triangles) around Figure 2.6 represent the direction of current. Recall Figure 1.7 and Figure 2.1 and notice that the circuit diagram of Figure 2.6 consists of those elements. Current must be parallel and opposite in direction to the electric field in order to get the current moving via electromotive force. The summation of voltages across the circuit must net to the total voltage drop or potential. Using Kirchhoff's circuit theory and Ohm's Law, the voltage across the circuits in Sections 2.5.1 and 2.5.2 can be theoretically determined among other potentials. It may be possible that the overall potential drop can have the appropriate attenuation applied via Equation (2.10).

Kirchhoff's theory is not well developed for this application to pipelines due to the ambiguity of several parameters compared to the Laplacian aspects that allow some boundary conditions per the attenuation methodology from the previous Section 2.4. To determine the summed resistance components shown in Equations (2.15) through (2.19) and per Figure 2.6 and Figure 2.7, actual field measurements need to be performed on a buried CP coupon and test stations along a pipeline in addition to CP ILI tool measurements.

Field test surveys (manual measurements) combined with the CP ILI tool data may help finding solutions in the analyses from Sections 2.6.1 and 2.6.2 below. This topic holds merit to extend to experimental research objectives outside of this study; however, may further validate methods from Section 2.4, ATTENUATION (see also Section 4.2).

2.6.1. Circuit of General CP System. This section uses Kirchhoff's method to illustrate the idea of summing the resistances around the circuit. This method has not been proven in industry experimentally.

(2.15)

$$\Delta \vec{V}_{tot} = \Delta E = (E_{cathode} - E_{anode}) = \Delta \vec{I} * \sum R,$$

R_0 = resistance of coating

R_1 = resistance of wire leads of rectifier

R_2 = resistance of anode wire leads

$R_3 = \sqrt{R_4 R_I}$; = soil resistance (electrolyte – see tables)¹⁷

(2.16)

$$R_4 = \frac{L}{kA} = \rho \frac{L}{A} = \text{longitudinal resistance of pipe,}$$

For area (L&P, eqn 4.41)¹ for model, $A = \pi * (OD * w. t.)$

$$\text{or by Laplace for a cylinder, } R_4 = \rho \frac{L}{A} = \rho \frac{\ln\left(\frac{r_2}{r_1}\right)}{2\pi kL}$$

$$k = \frac{1}{\rho} = \text{conductivity } \Omega * m^{-1}, \quad \& \quad \rho = \text{resistivity } \Omega m$$

The R_4 resistance is mainly a function of geometry through the arrangement of the conductivity of steel denoted by k and the inner and outer radii denoted by a lower case r for internal and external radii (diameter/2 = radius).¹⁷ Regarding Figure 2.6 this would mean that R_4 , R_3 and R_0 are in parallel; therefore the inverse of the three is necessary to attempt utilizing Kirchhoff's theory.

¹⁷ Griffiths, D.J. (1999). *Introduction to Electrodynamics, Third Edition*. Patparganj, Delhi 110 092, India: Pearson Education, Inc. Chapter 7.

The value of R_3 is provided in a table of resistances for soil, see the Appendix, and table 2-1 from the Air Force.¹⁸ Further the resistance Equation for a cylinder (tube) is critical to understand on the basis of Ohm's law. The resistance of the steel pipe above has some specific tabulated resistance values for various diameter pipes in $\mu\text{-Ohm}$ ¹⁹ as seen in the Appendix; however, this study only utilizes 12-inch OD per the supplied BHI data from the tool run on the sample pipeline, see Figure 2.6.

(2.17)

$$\begin{aligned}\Delta\vec{V}_{tot} &= \Delta\vec{E}_x = \Delta\vec{I}_x (R_0 + R_1 + R_2 + R_3 + R_4) \\ \Rightarrow \Delta\vec{V}_{tot} &= \Delta\vec{E}_x = \Delta\vec{I}_x \left(R_1 + R_2 + R_3 + \left(\frac{R_4 * R_0}{R_4 + R_0} \right) \right)\end{aligned}$$

Units: $V = \text{Amp}\Omega$

Therefore the potential of the pipe-to-soil is the following expression per Ohm's Law and Kirchhoff's method. There is ambiguity using Kirchhoff's methods since the length and gauges of wires for leads out to the anode and from the pipe to the rectifier are unknown as well as the length of the pipe.

Figure 2.5 and 2.6 demonstrate that Kirchhoff's theory would constantly change as the designated length of the pipe changes. To use this method, a specified length must be input to a model and boundary would conditions apply. This requires Laplace methods for the electric field gradient; therefore integration over the pipe distance. Notice that the resistance in parallel will get larger over distance. When $R \rightarrow \infty$ with length, then $I \rightarrow 0$, as per Ohm's Law.

¹⁸ Headquarters, Department of the Army (1985). *Electrical Design, Cathodic Protection*. No. TM 5-811-7 (Technical Manual Submerged Structures), Chapter 1, Washington D.C.

¹⁹ Department of Defence (2003). *Operation and Maintenance: Cathodic Protection*. UFC-3-570-06, Chapter 2-1 (Corrosion Cell), CP Design.

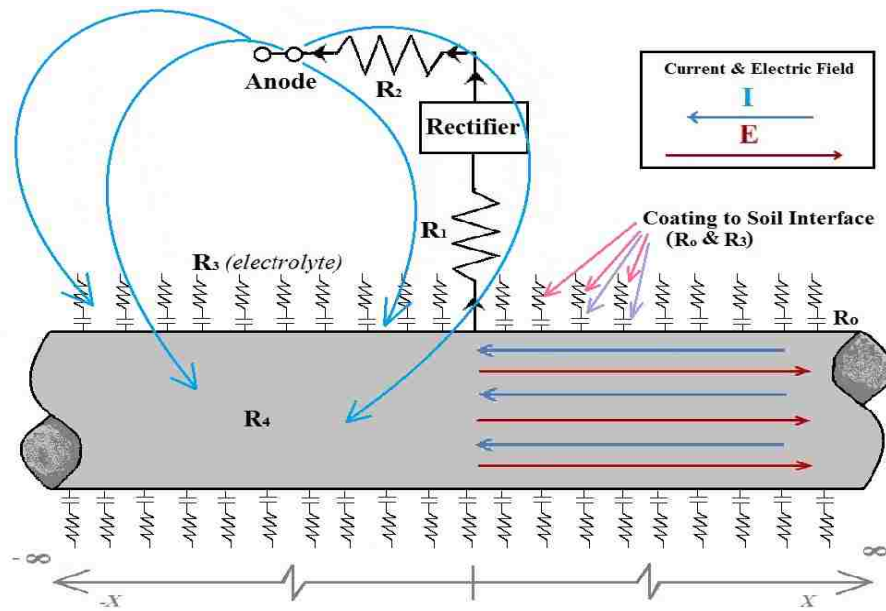


Figure 2.5 – Circuit Diagram of Cathodically Protected Pipe (a.)

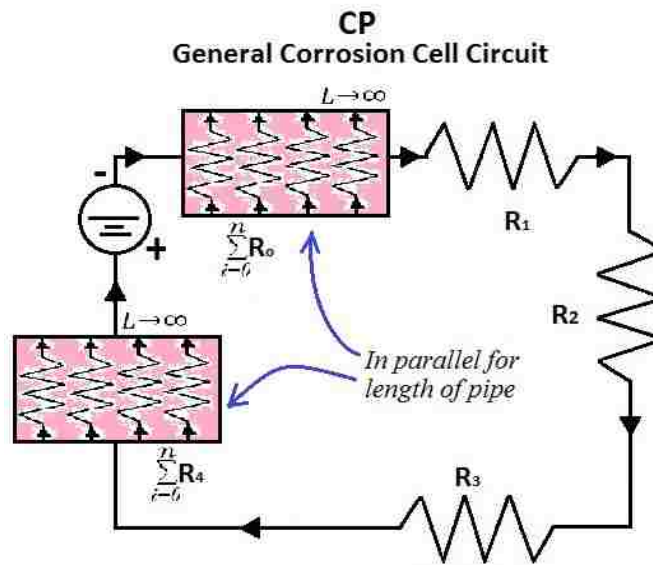


Figure 2.6 – Circuit Diagram of Cathodically Protected Pipe (b.)

2.6.2. Circuit of CP System with ILI Inside of Pipeline. This is Ohm's Law and Kirchoff's theory used in Figure 2.7. The arrows above the variables indicate that these are vector terms, consisting of both magnitude and direction. The tool is polar in nature thus impacting the vector direction at times with respect to the current flow and electrical field (potential).

$$\vec{V} = \overline{\Delta E} = \psi = \vec{I} * \sum R$$

The only difference in this diagram is the addition of the ILI tool into the circuit; therefore, another resistance is included in Kirchoff's theory. Recall R_5 from the ANALYTICAL VIEW PER CP ILI in Section 2.5. To determine the summation of the resistances around the circuit (corrosion cell) and to complete the circuit, the tool's resistance R_5 is required to be included as described in the introduction which expanded the diagram from Figure 2.6 to look like the new schematic of Figure 2.7.

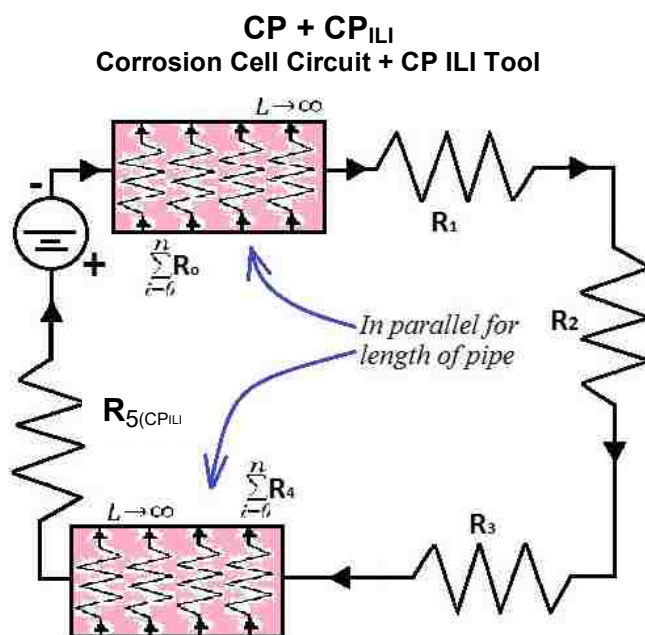


Figure 2.7 –Circuit Diagram of CP Pipe with ILI Measurement from Inside

While assuming attenuation still applies, notice that ΔE_x can be substituted into Equations (2.10) and (2.14). To find the potential E_o at the drain point, field test measurements at CP coupons must be performed and, based on coating efficiency²¹, may allow a basis to establish I_o and the rest can be found by the means of Kirchhoff's law.

(2.18)

$$\begin{aligned}\Delta \overline{V}_{tot} &= \Delta \overline{E}_x = \Delta \overline{I}_x \left(\mathbf{R}_1 + \mathbf{R}_2 + \mathbf{R}_3 + \left(\frac{\mathbf{R}_4 * \mathbf{R}_0}{\mathbf{R}_4 + \mathbf{R}_0} \right) + \mathbf{R}_5 \right) \\ \Rightarrow \Delta I_x &= \frac{\Delta E_x}{\sum R} \cosh(a_{att} (L - x))\end{aligned}$$

Since the desire is to find the total IR drop this Equation must be rewritten once more and then the natural log must be applied. When the natural log is in place, then those identities can be utilized. Recall Equation (2.14) as well for the resistance of the ILI tool and the substitution for ΔI_x .

$$\begin{aligned}\Rightarrow \Delta E_x &= \frac{2 * \Delta I_x \sum R}{e^u + e^{-u}} \\ \Rightarrow \ln(\Delta E_x) &= \ln \left(\frac{2 * \Delta I_x \sum R}{e^u + e^{-u}} \right) \\ \Rightarrow \ln(\Delta E_x) &= \ln \left(2 * \Delta I_x \sum R \right) - \ln(e^u + e^{-u}) \\ \Rightarrow \ln(\Delta E_x) &= \ln \left(2 * \Delta I_x \sum R \right)\end{aligned}$$

(2.19)

$$\therefore \ln(\Delta E_x) = \ln \left(2 * \Delta I_x * \left(\mathbf{R}_1 + \mathbf{R}_2 + \mathbf{R}_3 + \left(\frac{\mathbf{R}_4 * \mathbf{R}_0}{\mathbf{R}_4 + \mathbf{R}_0} \right) + \mathbf{R}_5 \right) \right)$$

The Equation above denotes the total logarithmic potential across the circuit including all resistance aspects summed. Theoretically all of the analyses for the attenuation and Ohm's law produce results given applicable data; however, the ambiguity

of Kirchhoff's methods may need further analysis that takes this research beyond its scope. There are field measurements that can be taken from CP coupons (test stations) to help fill in the listed resistances to these Equations (2.18) and (2.19) to produce measureable results; however, this thesis did not include a longer duration for additional experimental field data. Perhaps this method could help verify what the CP ILI tool is measuring and then being converted to potential.

All of the applicable methods from this entire Section 2 were utilized to establish a mathematical model in order to match up with the CP ILI device's data in the following Section 3.

3. CP ILI DATA & MODEL RESULTS

3.1. DATA FROM CP ILI TOOL

This section contains results from the engineering analysis in the previous section by using real world sample data from a CP ILI tool that performed a reading (called a tool run or smart pig run) gathered from a pipeline with respect to the conceptual diagram presented in Figure 2.7. The following ILI tool plots listed in Table 3.1 are for current vs. distance. The differences in the plots are due to the sample, the ILI reading sizes, over the listed distances. The data was provided by BHI and analyzed in conjunction with a Shell SME (part patent holder). The sample data for the three sets (Figure 3.1–Figure 3.3) is from different sections of a 12-inch nominal pipe diameter; 0.5-inch w.t.; 3.14ft (or 0.957m) circumference, and the area is of 1-ft length of pipe, which is 0.957m by 0.3048m equals 0.292 m². 20 Due to the limitation of data samples, per Table 3.1 and plots, it is difficult to tell if trends are linear, logarithmic or exponential because the change is so small; therefore, an estimated linear approximation was assumed.

Table 3.1 – List of CP ILI Data Sets with Sample Reading Size per Distance

CP ILI Data Set #	CP ILI Sample Size (cm)	CP ILI Avg. Current Density Amp/m ²	Segment Approx. Distance (m)	Figure
1	0.5	0.002	42.7	3.1
2	10	0.001 to 0.0017	6,401	3.2
3	10	0.00099 to 0.00169	6,797	3.3

3.1.1. CP ILI Data Set #1. The data sampling from the first data set in Figure 3.1 was for every 0.5cm. The plot shows a linear decline in current possibly indicating that

the tool is moving away from the rectifier (drain point) at -0.006 Amps/ft or -6.0 milliAmp/ft.²⁰ The trend line data is in the top right of plot. The random noise in the signal appears to be nearly one (1) Amp, which means the current drop, needs to occur over approximately 1,666ft to achieve a signal with as large of a magnitude as the noise seen in Figure 3.1.²⁰

A change of current of approximately 0.0006 Amps/ft is then 0.0006 Amps/0.292m² so 0.002 Amps/ m² or 2.0 milliAmps/ m² as observed from the plot.²⁰ This is reasonable for a pipeline with an assumed conservative 80% effective coating, from Equation (2.4).²¹

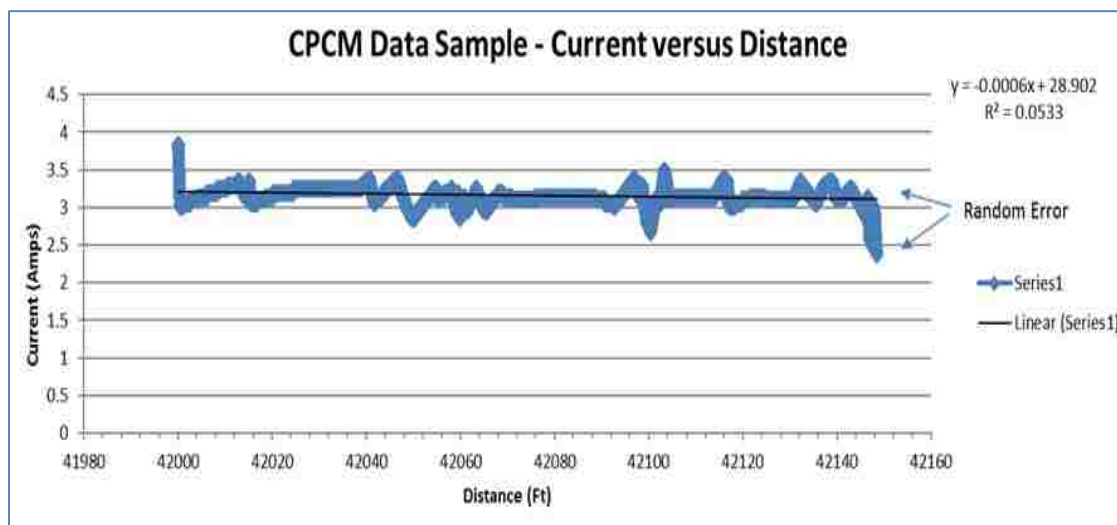


Figure 3.1 – CP ILI Sample Data Set 1, Plot

The range is acceptable upon consulting with SMEs in industry as to what is seen in the field and is representative of coating in good condition. As the CP ILI tool output

²⁰ Mateer, M. (2017, May 02). *CPCM Data Analysis Approach* [Telephone interview #3]. Discussions with Mark Mateer, Principal Asset Integrity Engineer

shows Figure 3.1, the specific current density value is ~ 2.0 milliAmps/m² at a coating efficiency ‘ η ’ of 80% for conservative measure.²¹

3.1.2 CP ILI Data Set #2 The next set of data from the CP ILI tool (Figure 3.2) on a different segment of the pipeline shows the current trend and a rectifier drain point. This data is sampled per each 10cm but it was not averaged over any distance with respect to noise. That is why there are more data points and more noise. There is a sudden change in current from one side of zero to the other at about 47,500ft. This is what a drain point looks like where the rectifier is attached to the line and the current direction makes a sudden shift. To the far left, the plot appears not to have a current reading, showing a value around zero; therefore, that region of pipeline is not receiving cathodic protection. This indicates an issue with the pipeline in that area, which must be addressed, meaning the CP system is down or compromised, etc. This research is not about assessing that particular pipeline; however, this is a positive result that the tool is able to detect variations in the readings.

“The plot shows the recorded current densities are reasonable for industry values ranging from 1.0 to 1.7 milliAmps/m², keeping within expectations for well coated pipelines. This data is essentially the same (within the margin of error) to the first data set, but they are not from the same section of pipeline.”²² It is hard to tell from the plot alone and may require field verification as it seems there is some interference or a fitting at the $\sim 37,000$ ft mark showing a drain-like effect and an increase.

²¹ Orazem, M.E.; Kennelley, J.K.; Bone, L. (1993). “*Current and Potential Distribution of a Coated Pipeline with Holidays, Part II – Comparison of the Effect of Discrete and Distributed Holidays*”, NACE Corrosion- Vol. 49, No.3.

²² Mateer, M., & Williams, D. (2017, May 02). CPCM Tool Data Plots. [Unpublished raw data]. Data from BHI; honed analytical process and approach by Mark Mateer.

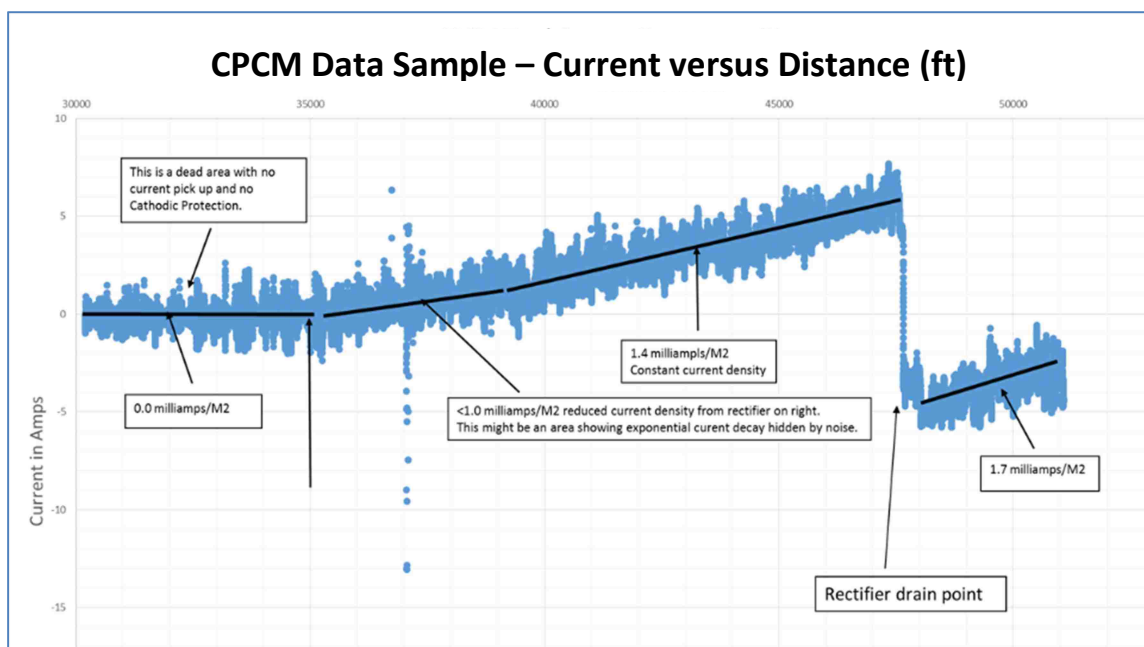


Figure 3.2 – CP ILI Sample Data Set 2, by Every 10cm

3.1.3. CP ILI Data Set #3 The third set of data had larger sampling points per every 10cm, instead of every 0.5cm. “There is noticeable noise, but the sampling still gives enough useful data. To dampen the noise, data points are averaged over each 20m and then plotted (Figure 3.3). Between two rectifiers there is always a mid-point or electric node point, where the current returns to one rectifier on one side of the mid-point and to the other rectifier on the other side of the mid-point.

The mid-point is at approximately 57,100ft. The exact mid-point is obscured by the noise, but to the left and right of the mid-point, current flows off the plot to other rectifiers and would jump from one side of zero to the other at the drain point.”²³

Another way to conceptualize what is happening with the data is through Figure 3.4 with

²³ Mateer, M. (2017, May 12). CPCM Data Analysis Approach on [Telephone interview #4]. Discussions with Mark Mateer, Principal Asset Integrity Engineer

some known electrodynamics. “The gradual change through zero is how it is determined that the mid-point is at approximately 57,100ft (Figure 3.3).”

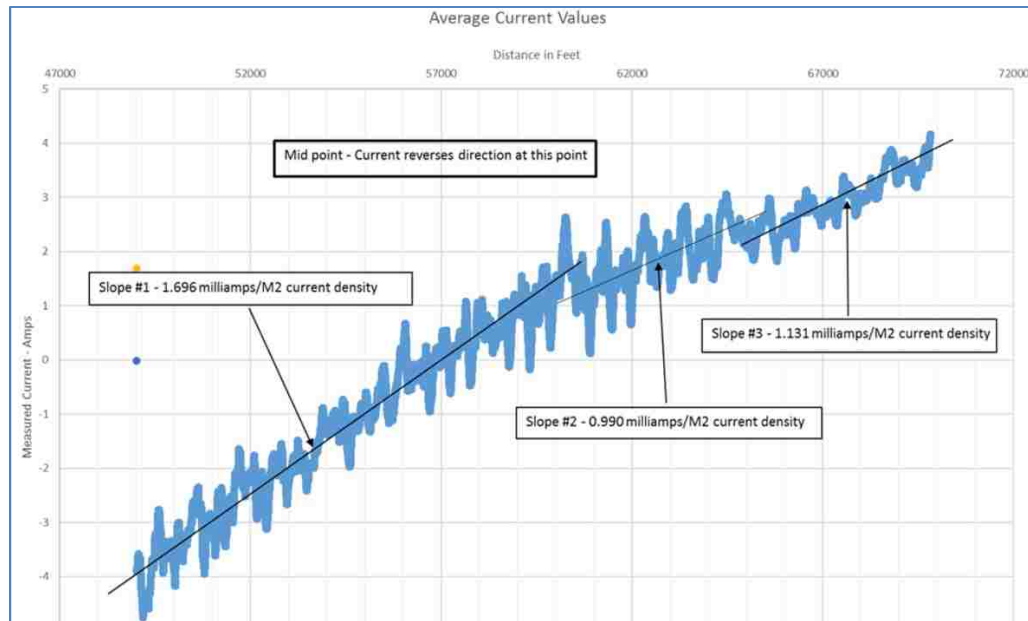


Figure 3.3 – CP ILI Sample Data Set 3, by Every 10cm

From the data in Figure 3.3, where the current changes direction it would appear to cancel out according to the physics as seen in Figure 3.4 (a) but that would not be correct; however, part (b.) of the figure is correct showing that the current is only entering on one side of the rectifier and then returning to the other side of the rectifier, appearing to have a more cyclic behavior.

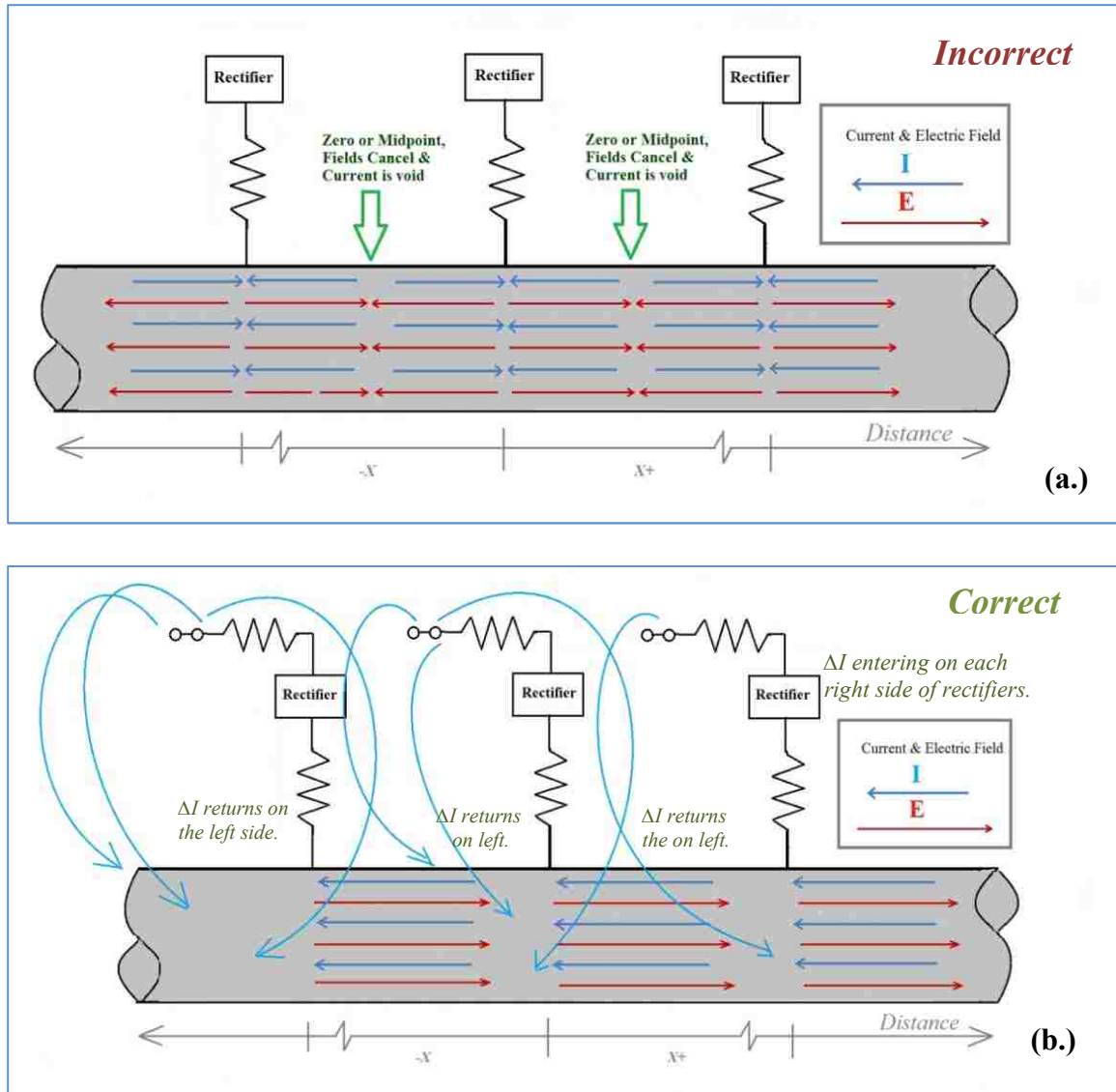


Figure 3.4 – Current Flow and E-field Conceptualization (Parts a. & b.)

3.2. MODEL RESULTS PER ENGINEERING ANALYSIS ON CP ILI DATA

This sub section is categorized with parameters for two different scenarios for the purpose of matching the three CP ILI tool data sets' current densities with the model. All of the calculations are based on an assumed distance of 7,620m (~4.75 to 5mi) between the rectifiers.

- a. First scenario (b) – The model parameters hold the over potential, Ψ_L , constant at -100mV and then vary the coating resistivity.
- b. Second scenario (0) – The model parameters vary for the over potential and then hold the coating resistivity constant at approximately 500,000 Ω m.

3.2.1. Constant Over Potential and Varied Coating Resistivity. For the first scenario parameters, this section includes corresponding figures on the following pages 47-53 for both the cathode potential and the current density attenuation curves. In general the following charts (Figure 3.5 through Figure 3.16) indicate that when the over potential is held constant and as the resistivity increases, both the attenuating current density and the attenuating cathode potential decline.

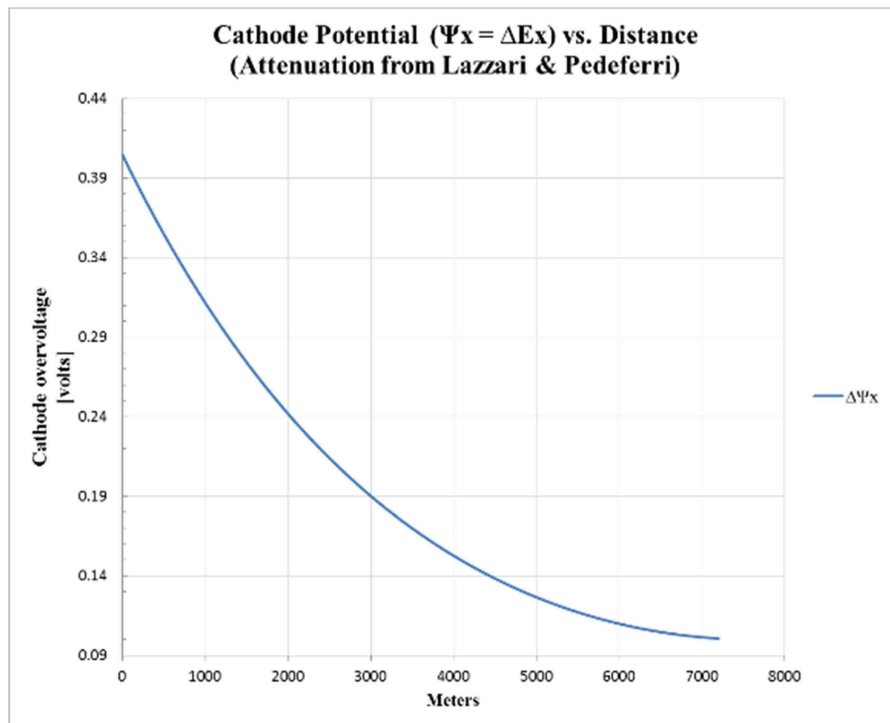


Figure 3.5 – Cathode ΔE_x Atten. @ Constant -100mV E_L (Data Set#1)

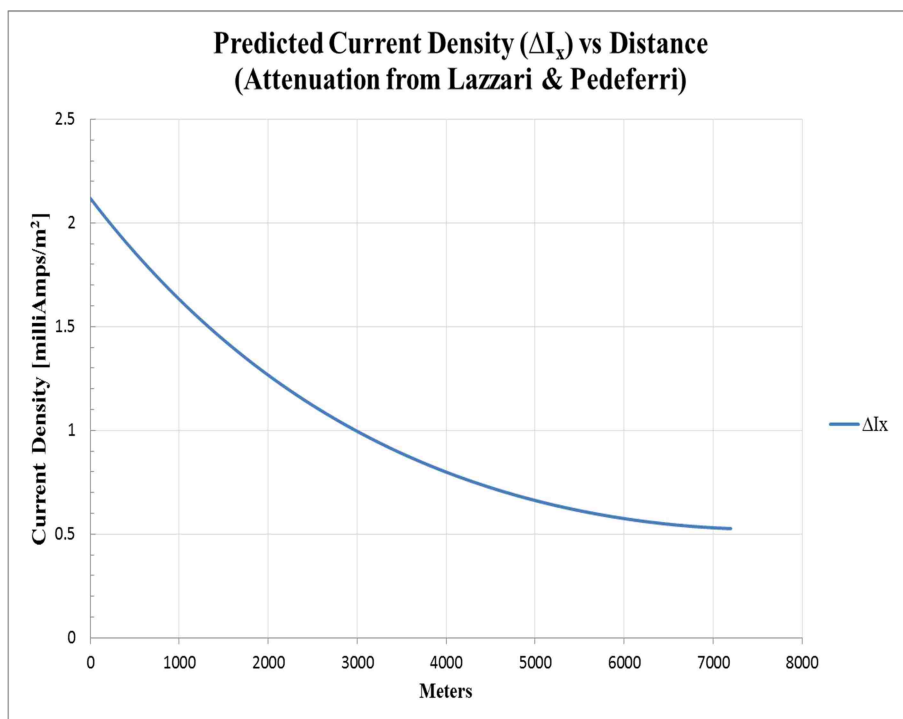


Figure 3.6 – Predicted ΔI_x at Constant E_L (Data Set#1)

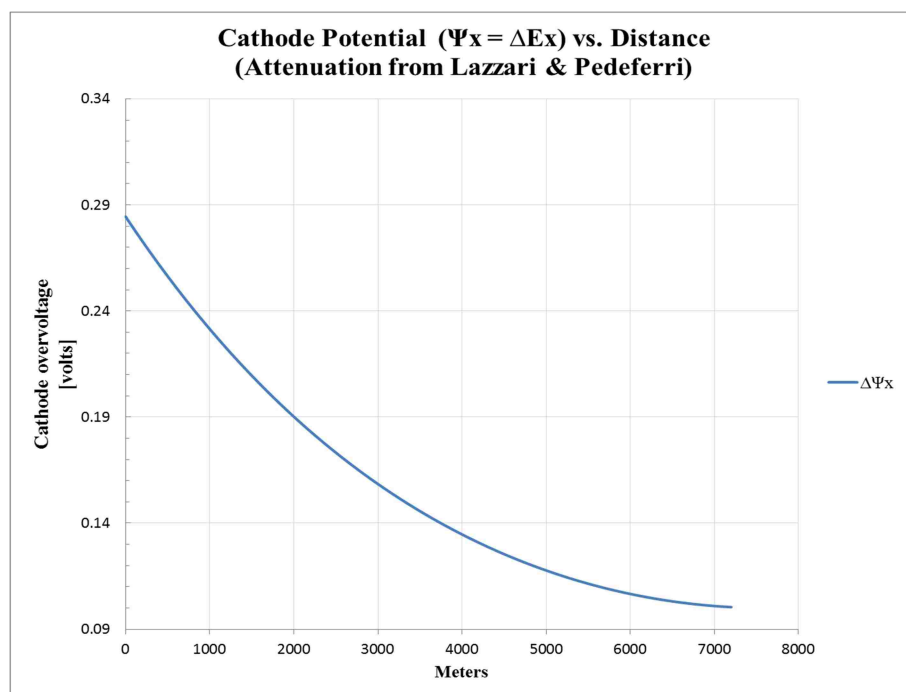
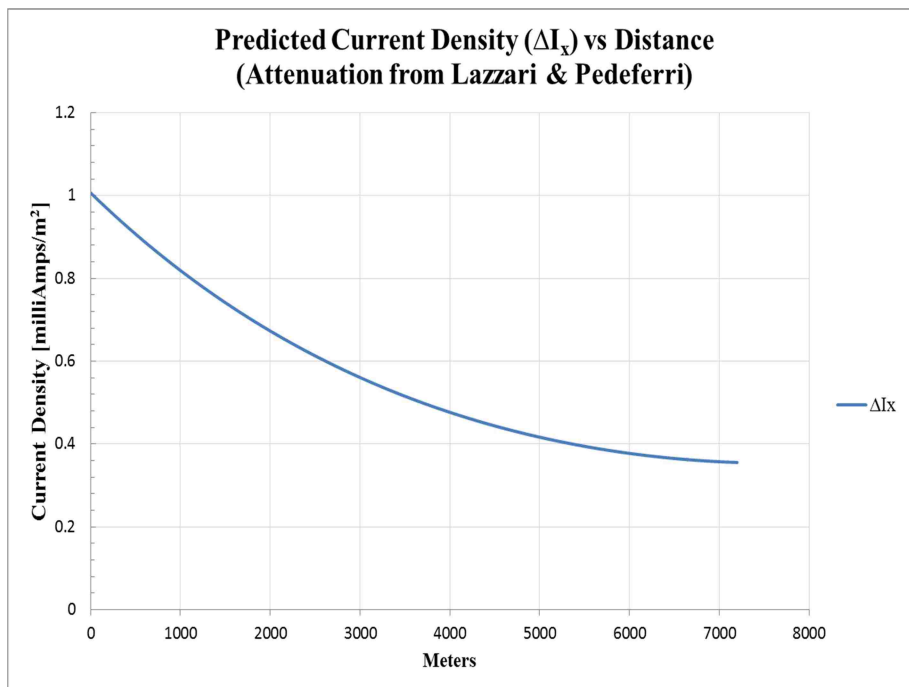
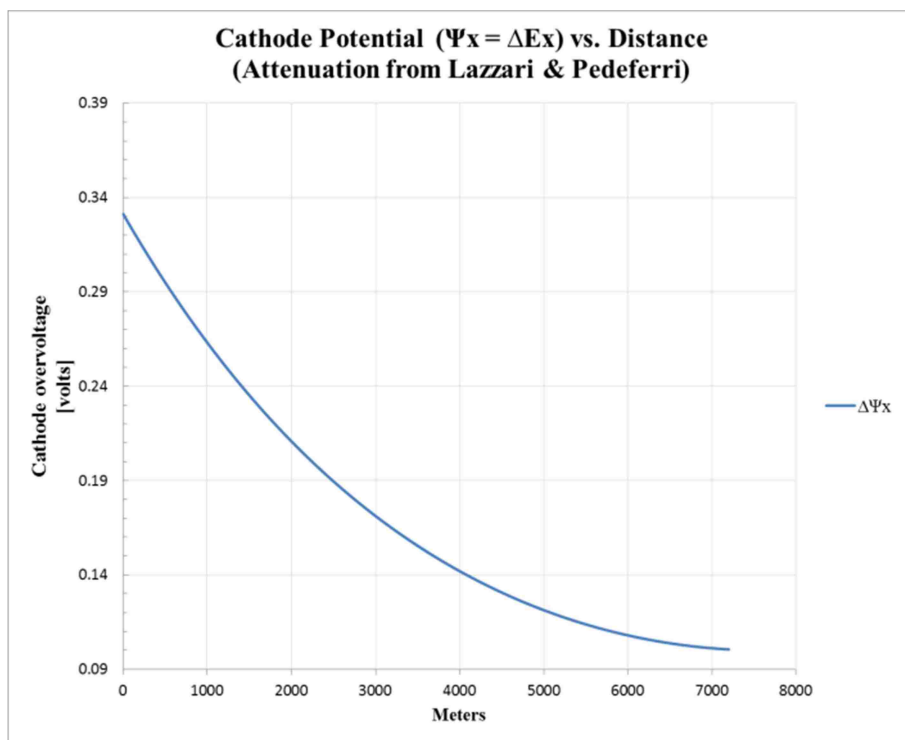


Figure 3.7 – Cathode ΔE_x Atten. @ Constant -100mV E_L (Data Set#2a)

Figure 3.8 – Predicted ΔI_x at Constant E_L (Data Set#2a)Figure 3.9 – Cathode ΔE_x Atten. @ Constant -100mV E_L (Data Set#2b)

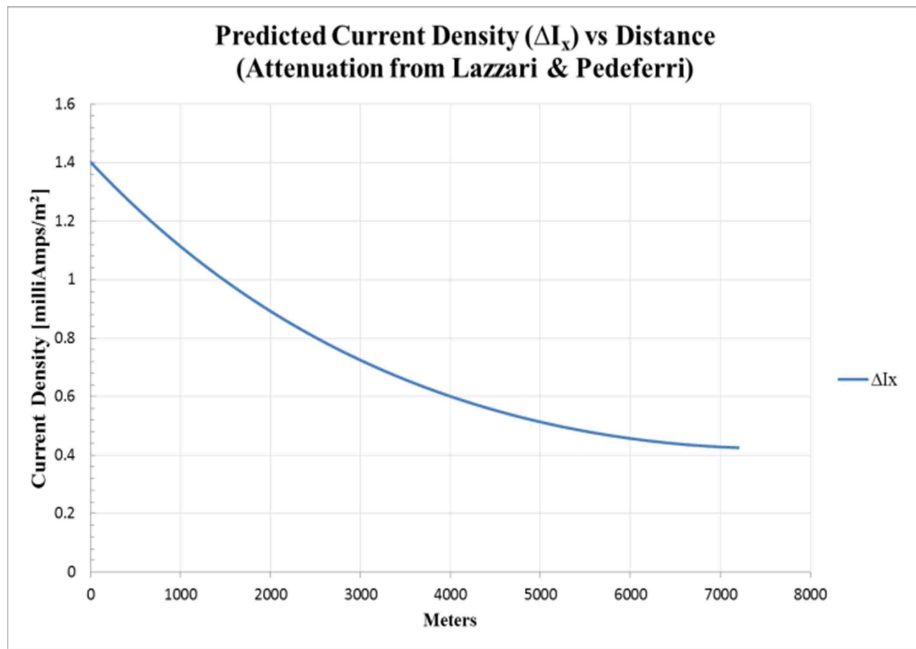


Figure 3.10 – Predicted Current Density at Constant E_L (Data Set#2b)

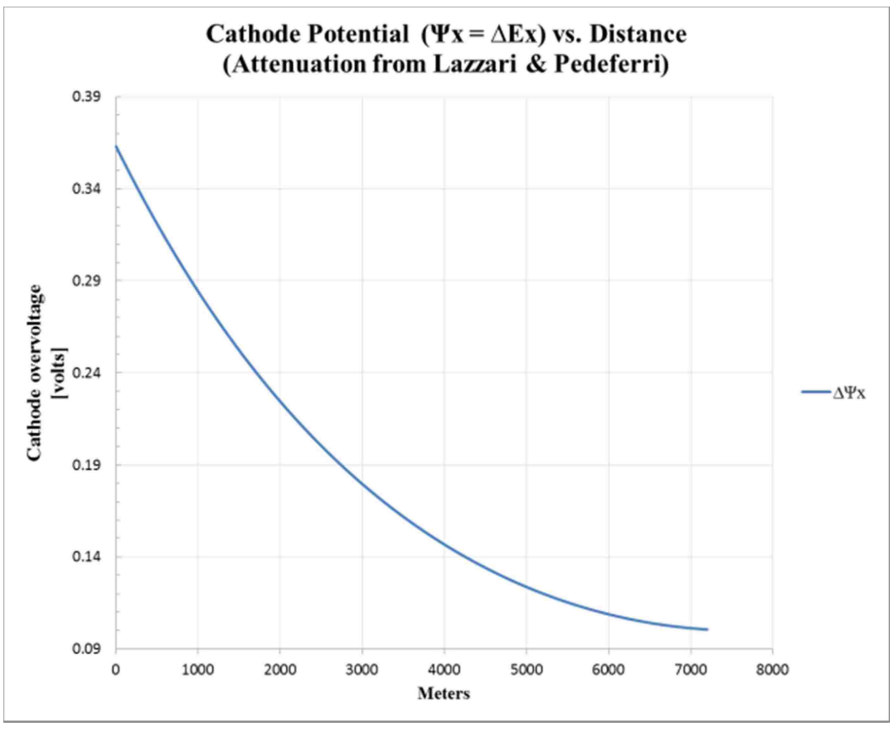


Figure 3.11 – Cathode ΔE_x Atten. @ Constant -100mV E_L (Data Set#2c)

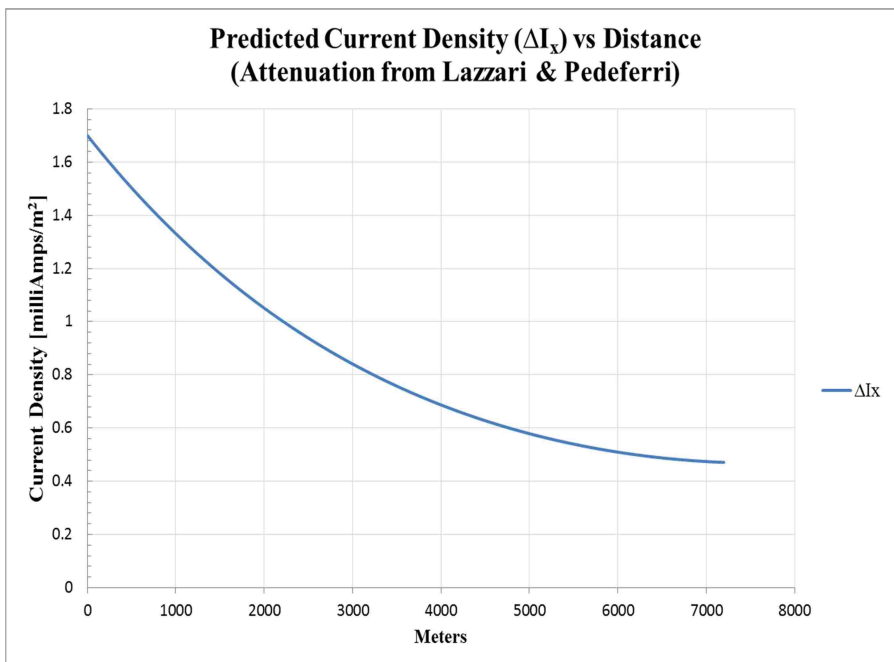


Figure 3.12 – Predicted ΔI_x at Constant E_L (Data Set#2c)

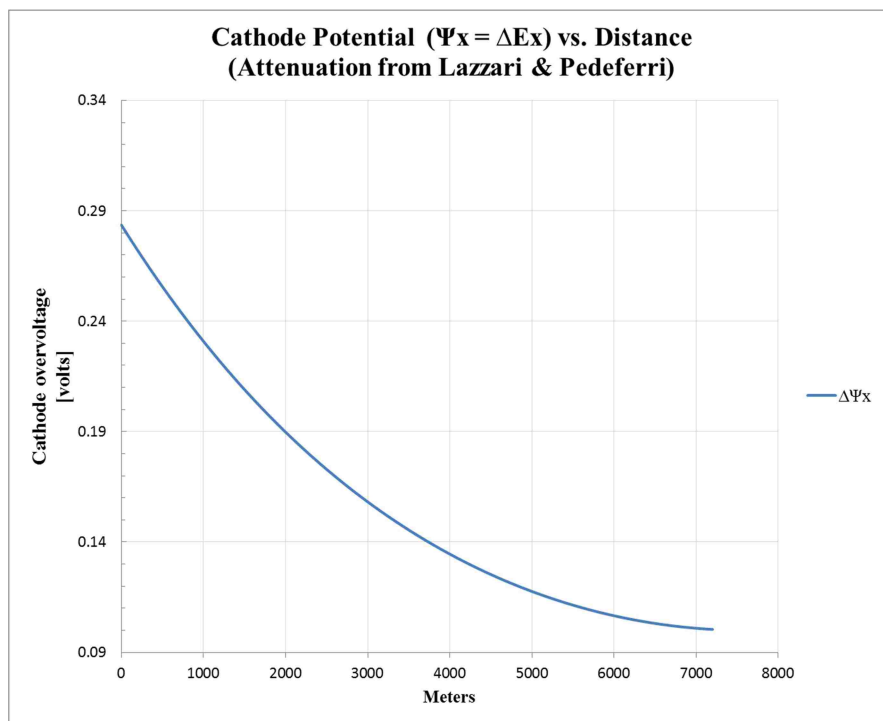


Figure 3.13 – Cathode ΔE_x Atten. @ Constant -100mV E_L (Data Set#3a)

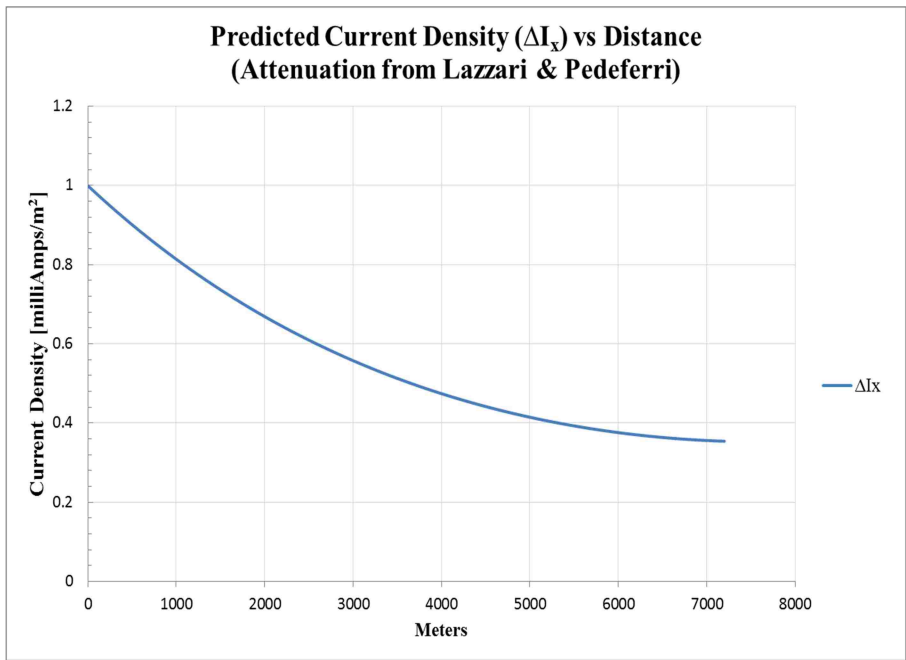


Figure 3.14 – Predicted ΔI_x at Constant E_L (Data Set#3a)

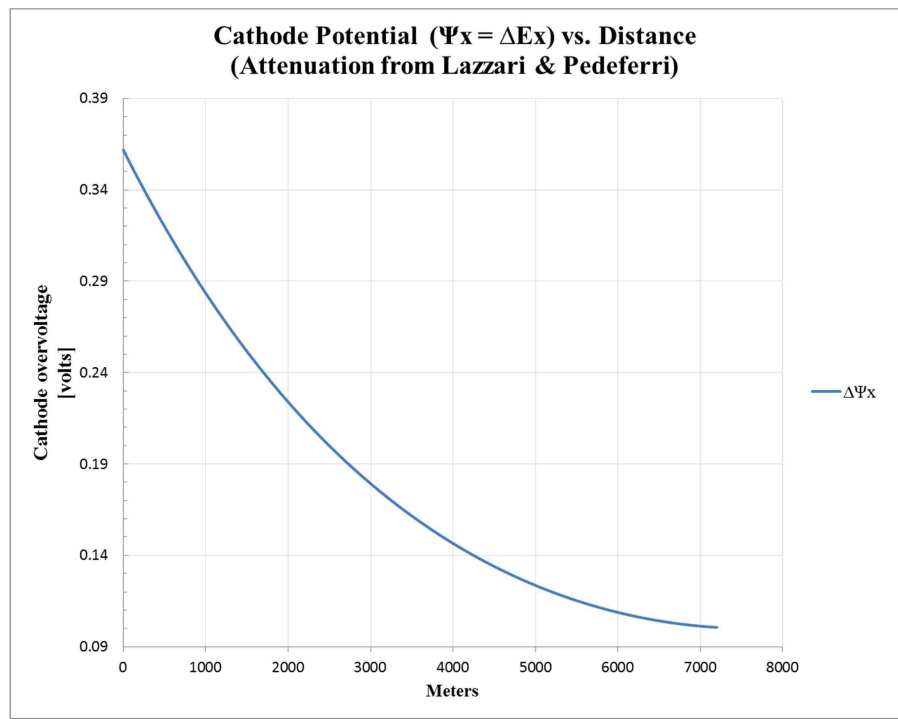


Figure 3.15 – Cathode ΔE_x Atten. @ Constant -100mV E_L (Data Set#3b)

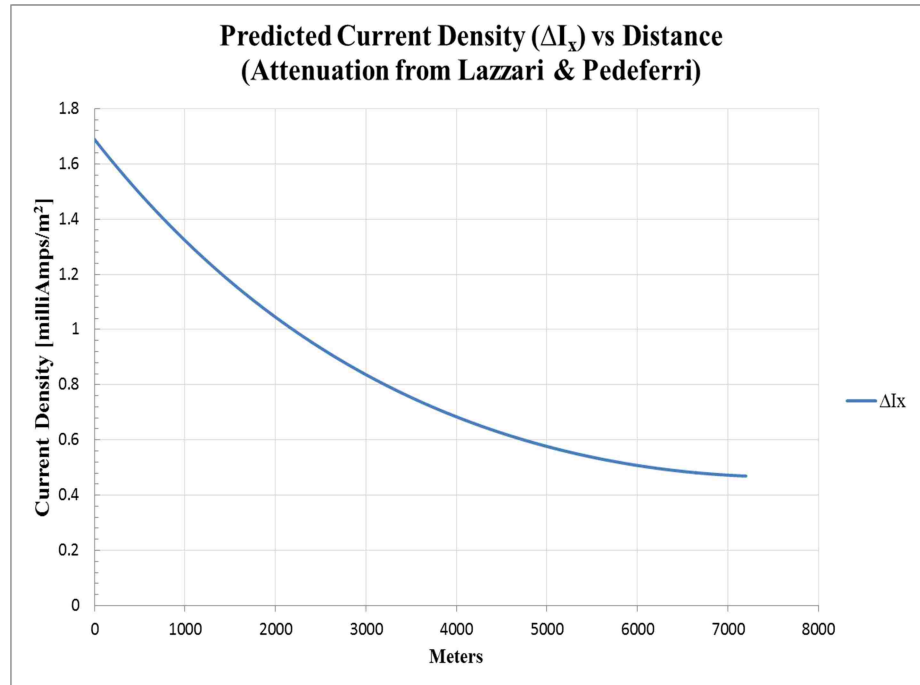


Figure 3.16 – Predicted ΔI_x at Constant E_L (Data Set#3b)

3.2.2. Varied Over Potential And Constant Coating Resistivity. For the second scenario parameters, this section will have the corresponding Figures 3.17 through 3.28 in the following pages 55-60 for both the cathode potential and the current density attenuation curves. These plots show when the coating resistivity is held constant at $500,000\Omega m$ in the model and as the over potential, Ψ_L varies (increases), both the attenuating current density and attenuating cathode potential increase. The trends of the plots will be further evaluated and discussed in Section 4.

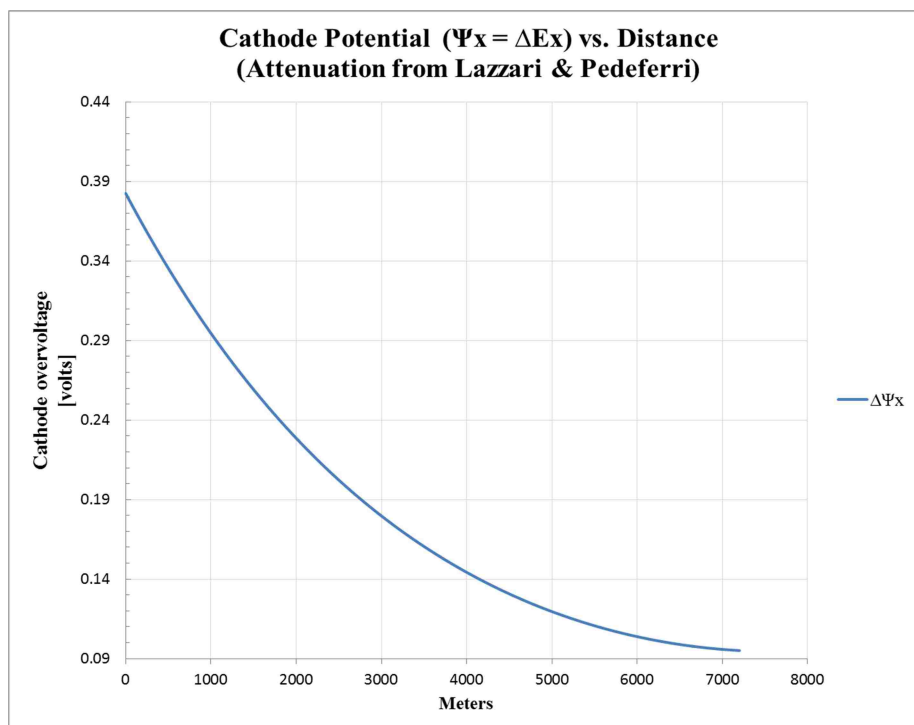


Figure 3.17 – Cathode ΔE_x Atten. at Varied E_L (Data Set#1)

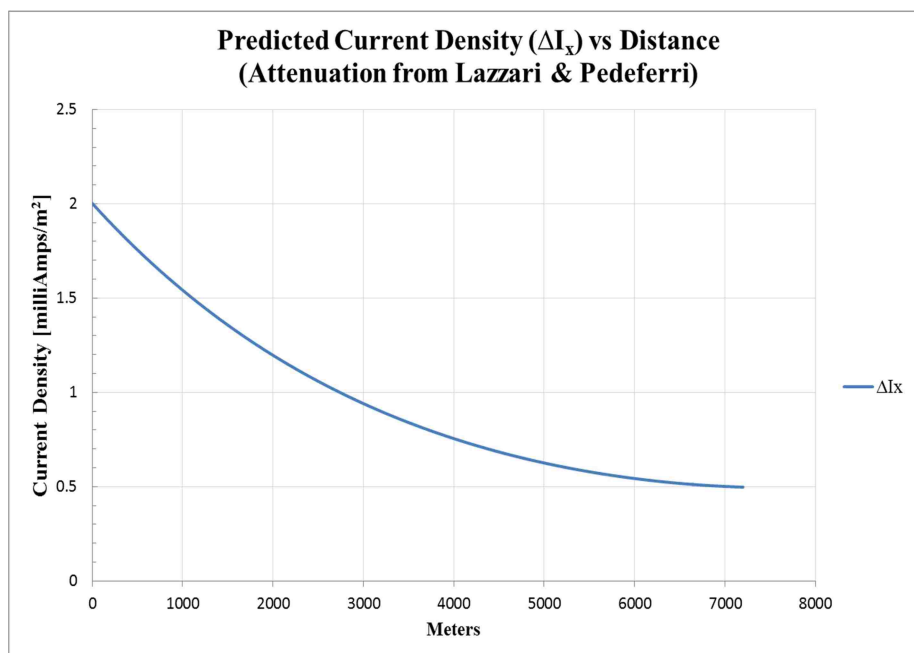


Figure 3.18 – Predicted ΔI_x @ Constant Coating Resistivity (Data Set#1)

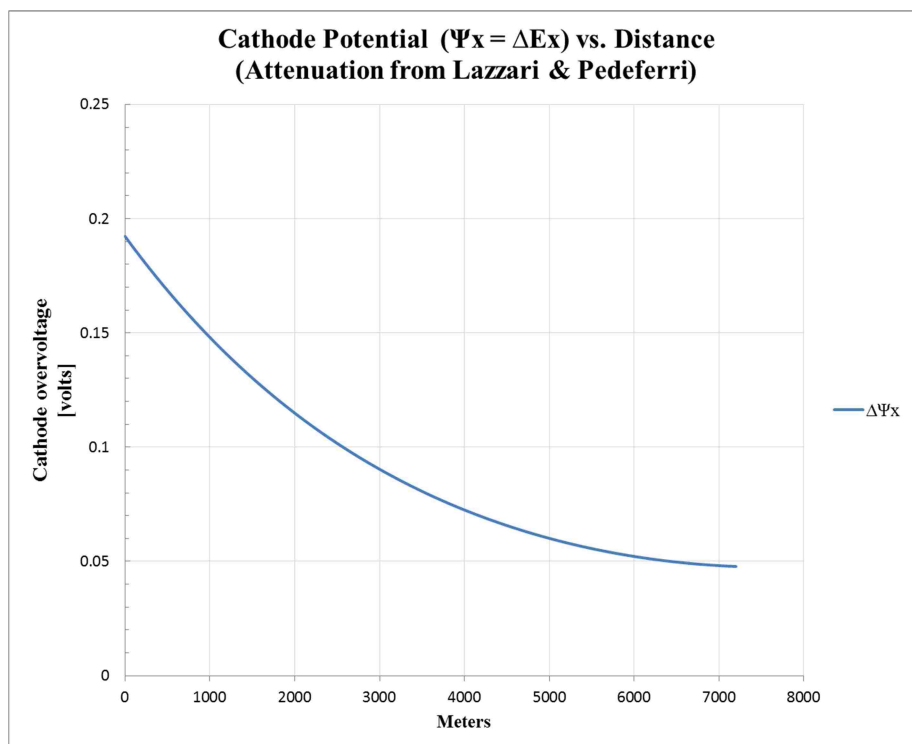


Figure 3.19 – Cathode ΔE_x Atten. at Varied E_L (Data Set#2a)

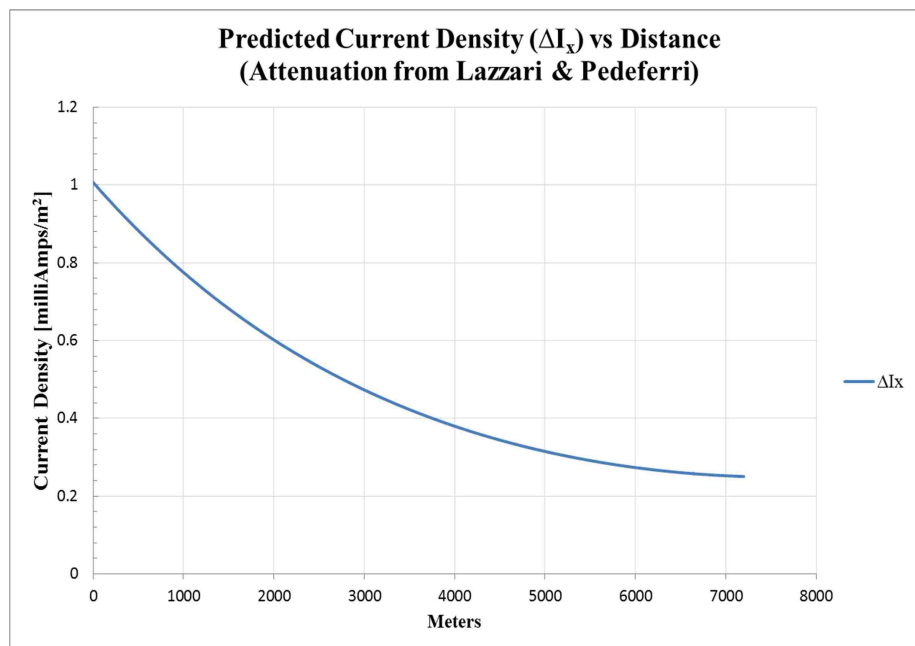


Figure 3.20 – Predicted ΔI_x @ Constant Coating Resistivity (Data Set#2a)

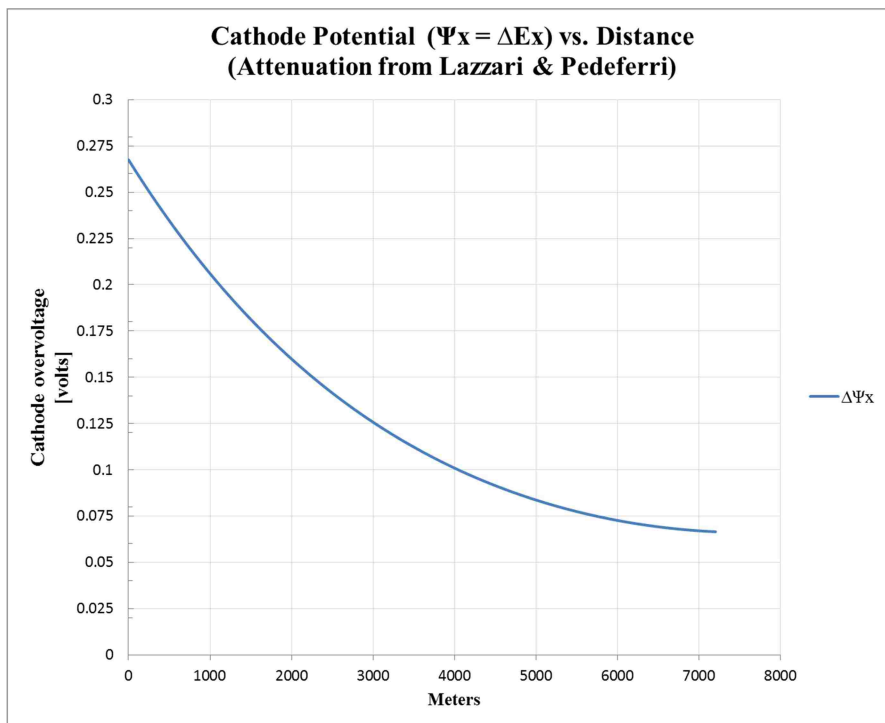


Figure 3.21 – Cathode ΔE_x Atten. at Varied E_L (Data Set#2b)

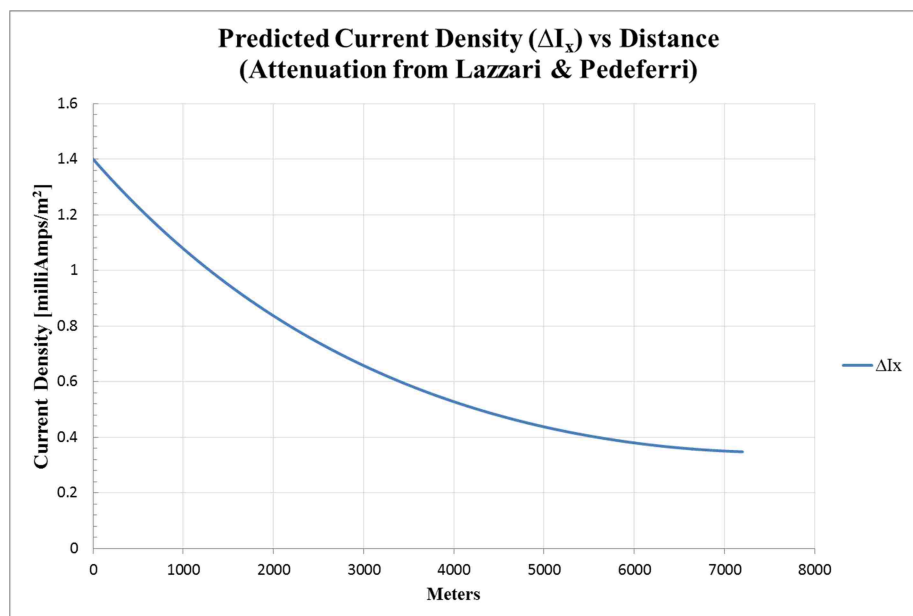


Figure 3.22 – Predicted ΔI_x @ Constant Coating Resistivity (Data Set#2b)

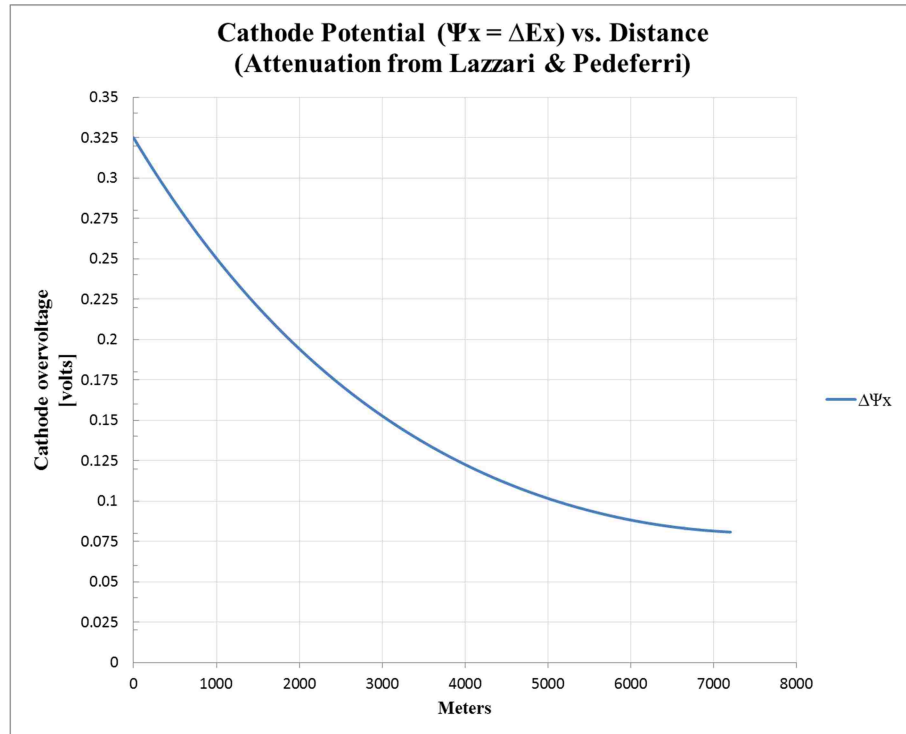


Figure 3.23 – Cathode ΔE_x Atten. at Varied E_L (Data Set#2c)

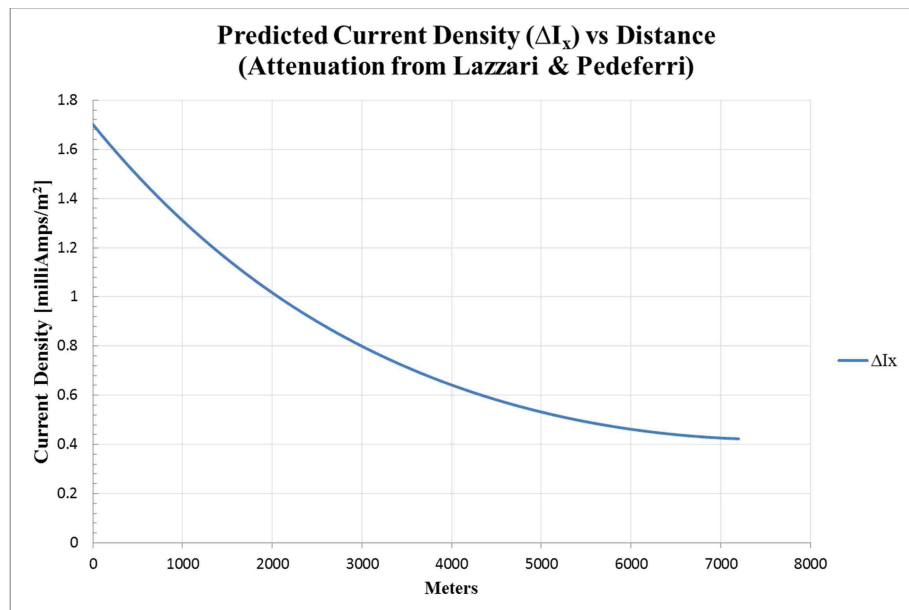


Figure 3.24 – Predicted ΔI_x @ Constant Coating Resistivity (Data Set#2c)

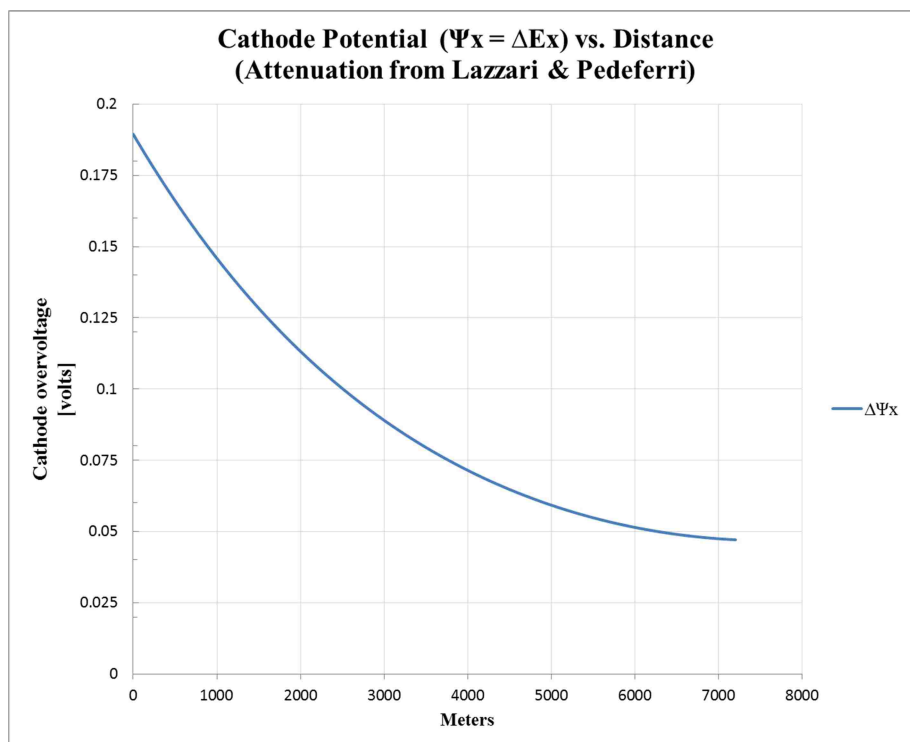


Figure 3.25 – Cathode ΔE_x Atten. at Varied E_L (Data Set#3a)

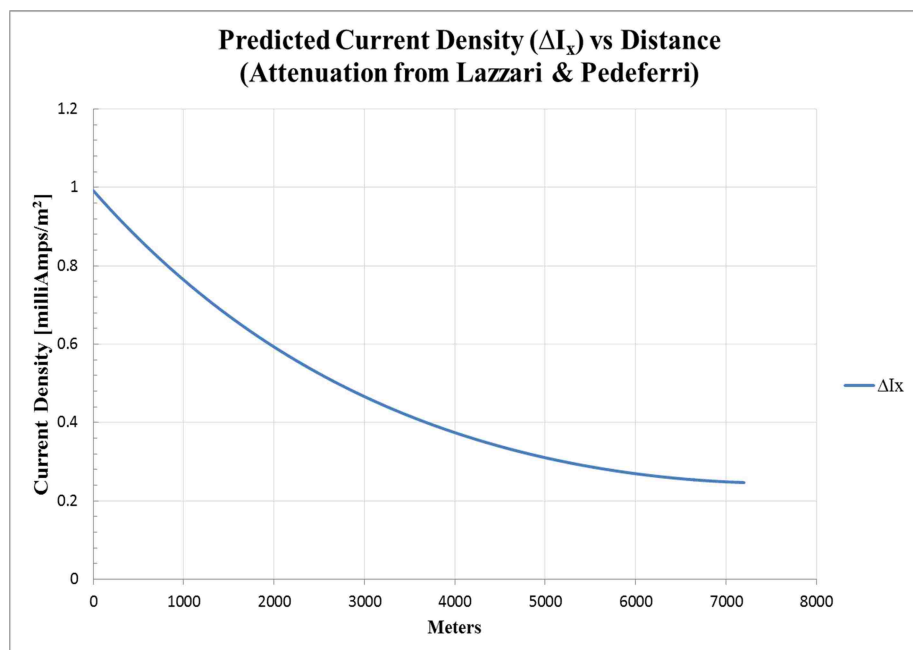


Figure 3.26 – Predicted ΔI_x @ Constant Coating Resistivity (Data Set#3a)

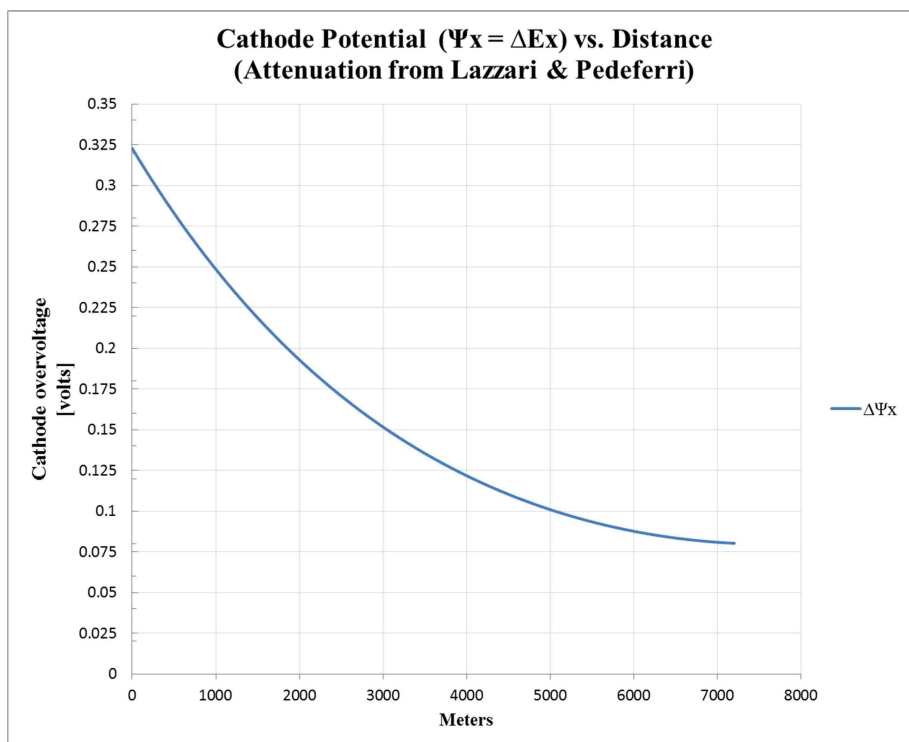


Figure 3.27 – Cathode ΔE_x Atten. at Varied E_L (Data Set#3b)

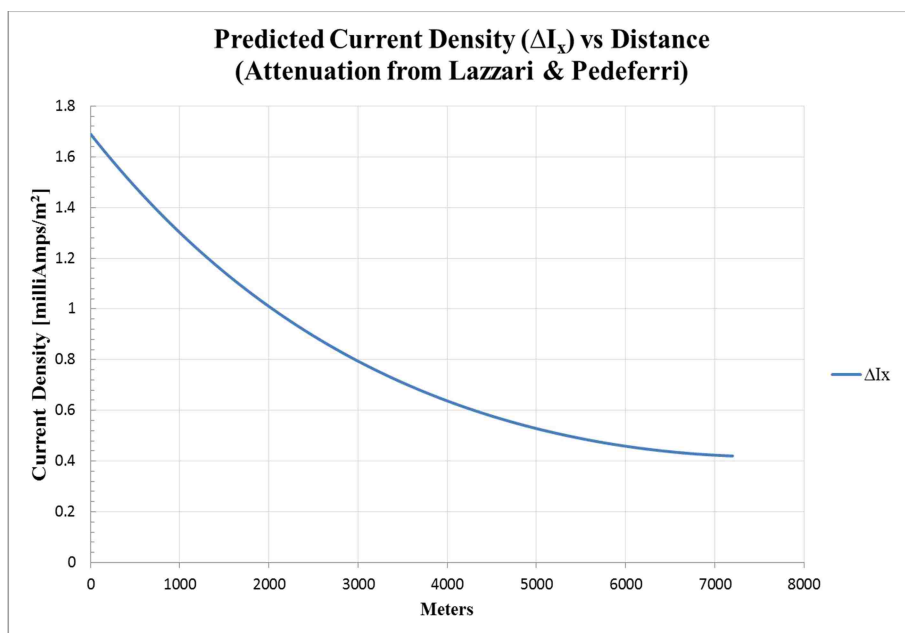


Figure 3.28 – Predicted ΔI_x @ Constant Coating Resistivity (Data Set#3b)

4. DISCUSSIONS AND CONCLUSIONS

The results from the attenuation model from the analysis show two apparent outcomes: 1) potential and 2) current, where the two are interrelated on the basis that the current can be calculated from the potential through Ohm's Law by simply adjusting the over potential or the transverse coating resistance values to achieve protected potential ranges. The model was able to match the CP ILI data for current density by adjusting the aforementioned values as seen in Table 4.1 and Table 4.2. From this perspective, it shows to be an electrical circuit calculation per Equation (2.14) with the attenuation methods and does not take chemistry and diffusion into account. However, the potential outputs achieved in this study are indicative that polarization is possible, therefore impacting the electrochemistry.

4.1. DISCUSSION – RESULTS OF GRAPHS & CHARTS

“Due to polarization from the calcareous deposits the potential and current density are independent of each other since current depends on the diffusion rate of oxygen, per Figure 1.3 – Lazzari and Pedferri (*L&P*), but the potential does not.”²⁴ The L&P model seems to assume that only coating resistance determines the current once the potential is known; however, from the polarization curves, it shows that potential and current are independent of each other once the cathode polarizes (recall Figure 1.3).

Figure 4.1 is a representation of how the model results (all plots) in the subsection for constant over potential behave. This assumes that the matched current density to the

²⁴ Mateer, M. (2017, May 23-30). CPCM Data Analysis Approach [Collaborations and Correspondence]. Discussions with Mark Mateer, Principal Asset Integrity Engineer

CP ILI tool is actually a maximum value and driven by the over potential; therefore, is the “impressed current” on the CP system.

Figure 4.1 and Figure 1.3 (explained in Section 1.2.1.3, page 9) have similarities, where the red line designates the CP ILI tool measurement and how it is believed the current demand may look. The diffusion limited area is the blue flat line where the pipe polarizes and then declines by hyperbolic cosine function where the CP system can no longer deliver sufficient current.²⁴ (i.e. Set#1, per averaging methods)

Figure 4.1 also shows theoretically the opposing curves for the supply of current density and the demand of current density. The result indicates that they balance each other out to a constant current density, thus a flat line. However, on the right end of the plot where the current density decays and the oxygen migrates to the surface because it is not consumed by the current, then calcareous deposit is inhibited.

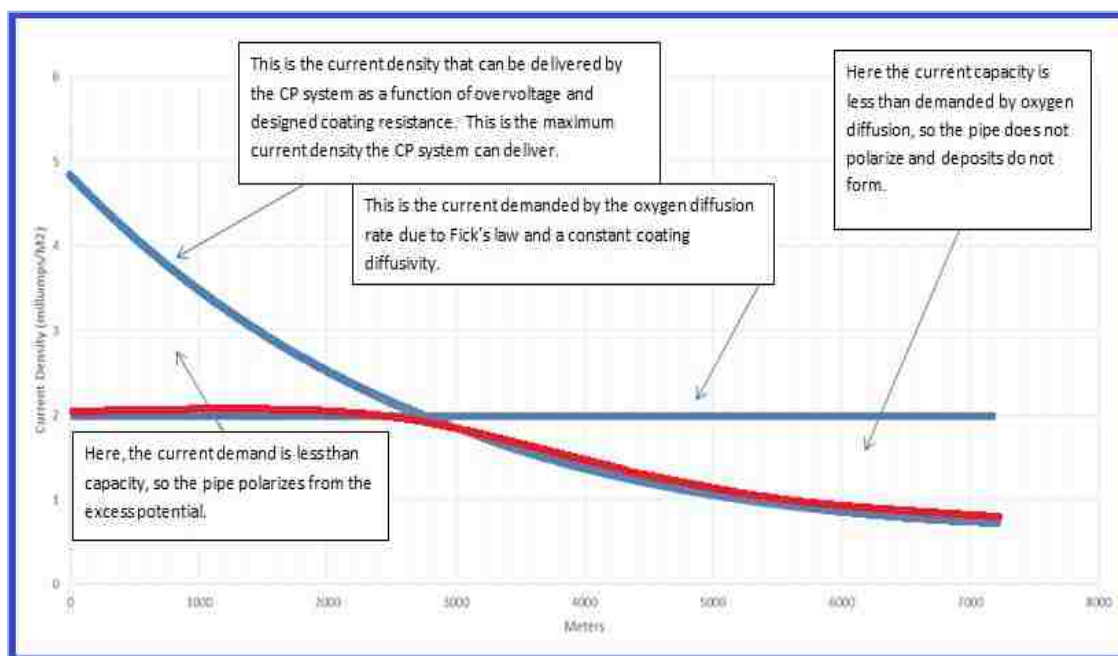


Figure 4.1 – Conceptualization of Data Observations

Table 4.1 summarizes the model results from the three data sets from BHI plotted in pages 47-53 for attenuating current density and the attenuating cathode potential. To correlate model values with the tool, the over potential was held constant and the coating resistivity inputs were varied. Regarding Table 4.1 data, where the over potential was held constant, -100mV, Figure 4.2 depicts that as the coating resistance increases then both the current density and cathode potential linearly decreases. A magnification of the scale of the potential is in Figure 4.3.

The next Table 4.2 includes the model results from the three CP ILI tool data sets which vary the over potential instead and keep the resistivity constant. The linear relationship from Table 4.2 point values conveys that as the over potential increased then both the attenuating current densities and cathode potentials increased. Consequently, in Figure 4.4, this further illustrates that the over potential is driving ΔI_x & $\Delta \Psi_x$.

Table 4.1 – Constant Over Potential ($\Psi_L = \Delta E_L$), “Midpoint” Voltage

CP ILI Data Set	Model Outputs ¹			CP ILI Data Current Density $J = \Delta I_x / m^2$ milliAmp/ m^2	Figures pages 48-53
	Constant Over Potential $\Psi_L = \Delta E_L$ mV	Varied Coating Resistivity ρ_o (Ωm)	Max. Cathode Potential Atten. $\Delta \Psi_x = \Delta E_x$ mV		
Set #1	-100	508,999	-398	2.0	3.5 & 3.6
Set #2a		740,000	-285	1.0	3.7 & 3.8
Set #2b		618,000	-331	1.4	3.9 & 3.10
Set #2c		559,000	-363	1.7	3.11 & 3.12
Set #3a		743,000	-284	0.99	3.13 & 3.14
Set #3b		561,000	-362	1.69	3.15 & 3.16

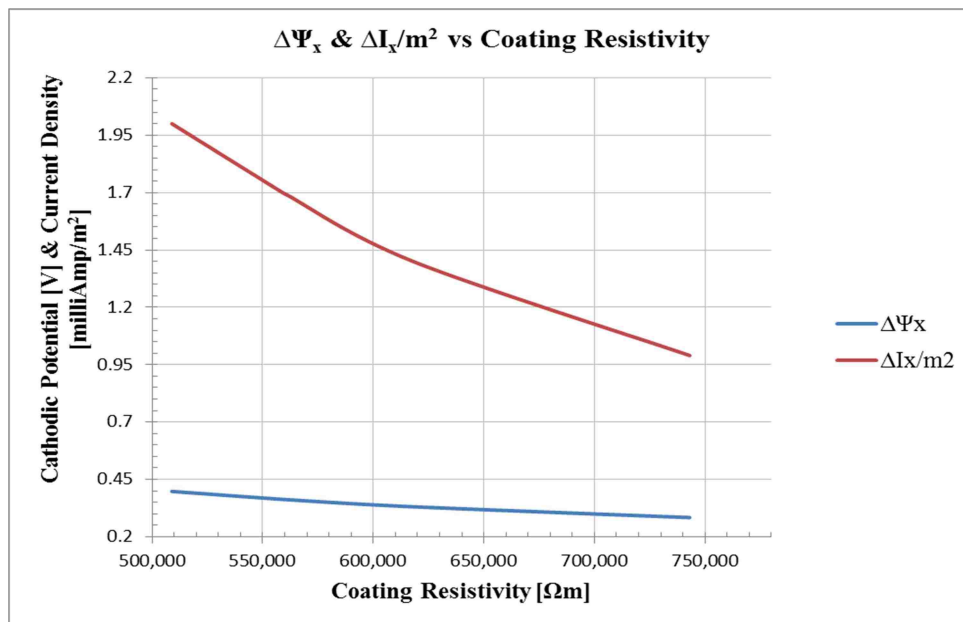


Figure 4.2 – Table 3.1 ΔI_x & $\Delta\Psi_x$ as Coating Resistivity Increases

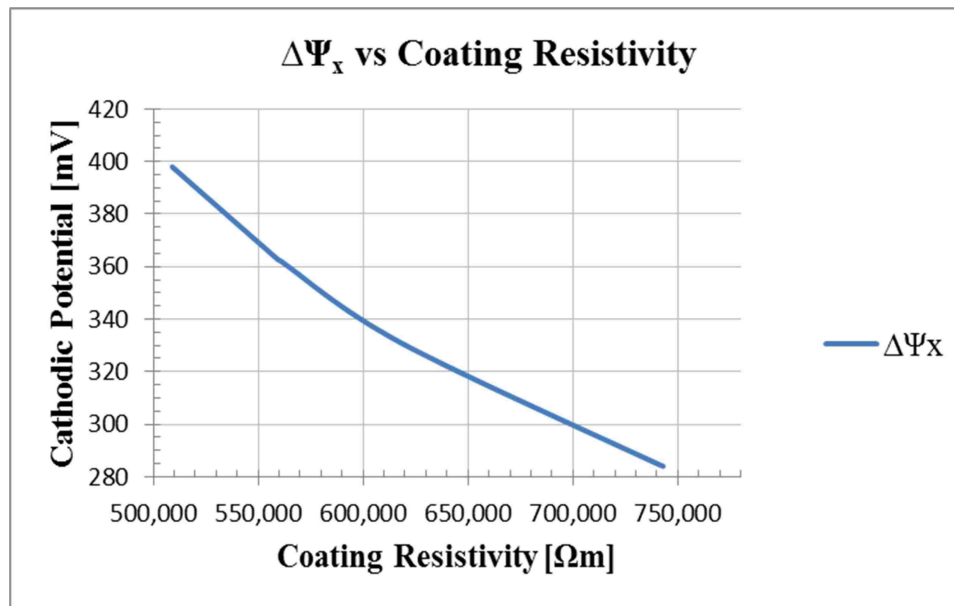
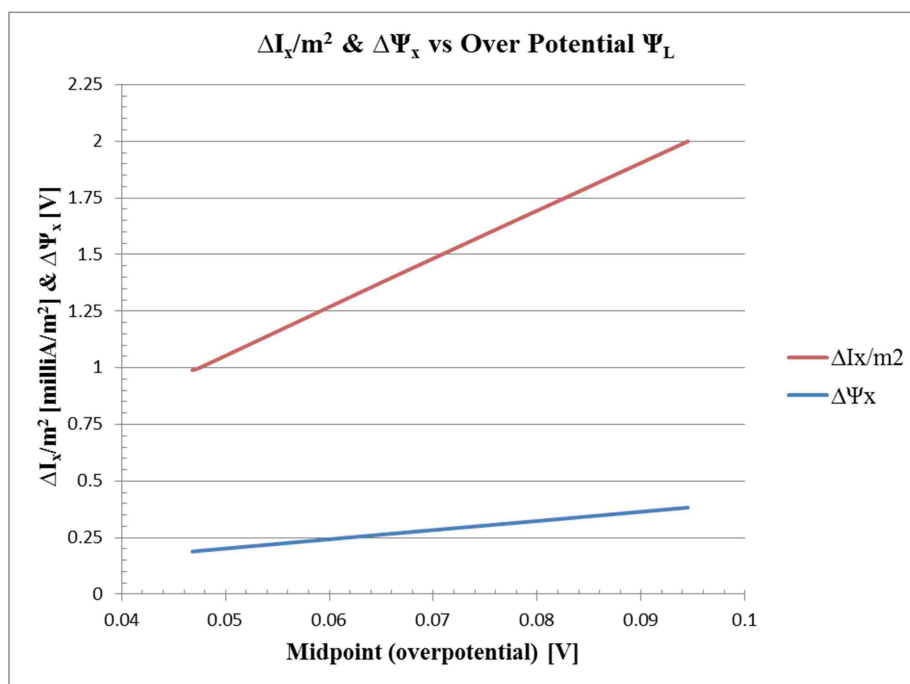


Figure 4.3 – Magnification of $\Delta\Psi_x$ mV (Fig. 4.2) as Coating Resistivity Increases

Table 4.2 – Constant Coating Resistivity Ωm

CP ILI Data Set	Model Outputs			Match to CP ILI Data Current Density $J = \Delta x I / \text{m}^2$ milliAmp/ m^2	Figures Pages 54-60
	Varied Over Potential $\Psi_L = \Delta E_L$ mV	Constant Coating Resistivity ρ_o in Ωm	Max. Cathode Potential Atten. $\Delta\Psi_x = \Delta E_x$ mV		
Set #1	-94.5	500,000	-383	2.0	3.17 & 3.18
Set #2a	-47.5		-192	1.0	3.19 & 3.20
Set #2b	-66.1		-268	1.4	3.21 & 3.22
Set #2c	-80.3		-325	1.7	3.23 & 3.24
Set #3a	-46.8		-189	0.99	3.25 & 3.26
Set #3b	-79.8		-323	1.69	3.27 & 3.28

Figure 4.4 – From Table 3.2 Data: ΔI_x & $\Delta\Psi_x$ Driven by $\Delta\Psi_L$

4.2. FINDINGS

Current attenuation does not seem to appear in the CP ILI data over a large distance with large potential attenuation as anticipated from the texts.¹ This method cannot work when current density is a function of the potential. “Current does not appear to be a function of potential in the “protected potential” range. The results demonstrate that due to polarization from calcareous deposit the potential and current density are independent of each other since current depends on the oxygen diffusion rate, where the potential does not.”²⁴

The CP ILI data and model results convey that oxygen diffusion controls the cathodic reaction and that the current will remain constant while the potential varies. The potential starts out high at the drain point and attenuates down, but the current remains constant since it is limited by the oxygen diffusion rate (Figure 4.1). The addition of calcareous deposits makes the effect larger as it limits the current even more and flattens out the polarization curve at lower potentials. It seems apparent that the potential can attenuate, but the current cannot if it is diffusion limited. From the results and discussions, the CP ILI data does not show current density to vary if the oxygen is diffusion limited.

The potential will move up and down the curve in the plot depending on attenuation, but the current doesn't change since the cathode line is vertical. From Figure 4.1 and Figure 4.5 and by Table 4.1 and Table 4.2, the data shows current density prediction in the attenuation model is the maximum current density that the CP system can provide. Where far enough from the drain point the current provided by the CP system can no longer meet the oxygen diffusion rate and current will drop (Figure 4.1 and

Figure 1.3). This is shown in the CP ILI chart with three different current densities as seen in Data Set #2.

When current flows from the rectifier, the cathode reaction at the pipe surface will produce excess OH^- (hydroxyl) ions,²⁵ which is the reduction of oxygen (Equation 1.6), which in turn will raise the soil's pH. This concept will be referenced as pipe-to-soil potential. "As the current flows, the cathode reaction is driven to the right with excised OH^- , thus increasing the pH in the soil causing precipitation of minerals over time called calcareous deposit."²⁰

The growth of calcareous deposit depends on current to make the electrochemical process occur. More deposit will accumulate in areas of high current versus low, namely the closer to the drain point. 10 & 24 Recall Equation (1.6), for oxygen diffusion, the calcareous deposit raises the R_o (coating resistance) to again slow the diffusion of O_2 to the pipe's surface (from Equation 1.3). Current depends on potential shift as illustrated in the applied attenuation principles from Section 2.4 and through Ohm's Law.

The coating resistivity R_o is critical in Equation (2.2) and From Ohm's Law the following relationship as established in Equation (2.8). Note that as R_o increases over time, the current will begin to fall and normalize, making a flatter profile as shown with the dotted line in Figure 4.5, which is the final new current profile. If R_o continues to increase closer to the drain point, then current will drop further, closer to zero, since the resistance is higher, and hence a flatter more stable current. This is indicative of a protected and polarized pipe, which is desirable in industry. From this analysis the CP

²⁵ Allahar, Kerry N.; Orazem, Mark E. (2009) "On the Extension of CP Models to Address Cathodic Protection Under a Delaminated Surface." Elsevier Ltd., University of Florida: Gainesville, FL.

ILI data will be attempted to be matched with to see if the current can achieve stability (constant) as shown Figure 4.5.

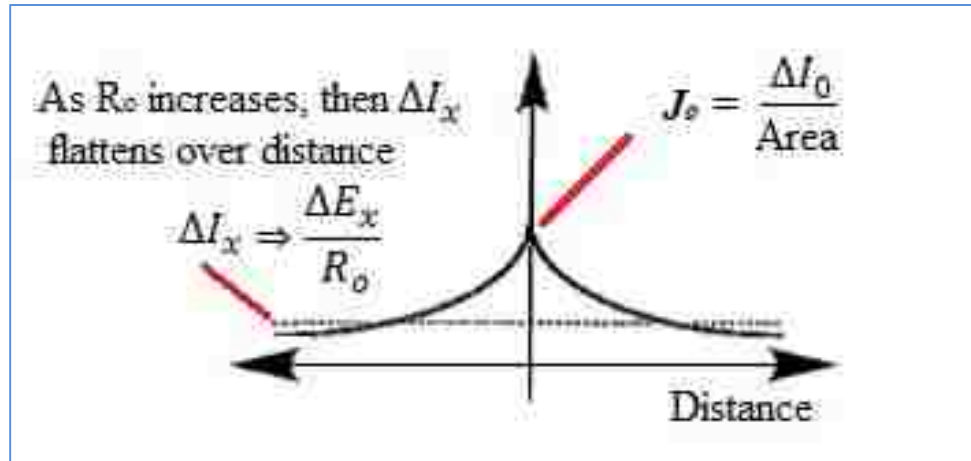


Figure 4.5 – Current Density at Drain Point and Normalized Current

4.3. CONCLUSIONS

This research is mainly an electrical circuit evaluation per Equation 2.14 with the attenuation methods and it does not directly relate to the electrochemistry and rate of diffusion. At the same time through using the model, the potential values as tabulated in Table 4.1 and Table 4.2 reveal that polarization is possible and in turn will impact the electrochemistry. The CP ILI data and model results from Section 3 exhibit that oxygen diffusion Equation (1.7) controls the cathodic reaction and that the current will remain constant while the potential and coating resistivity varies (see Table 4.1 and Table 4.2). The CP ILI data can be matched via Equation (2.14) in the model.

$$\Delta I_m = \frac{(E_1 - E_2)}{\left(\frac{\rho * L_{CPILI}}{(\pi * (r_{OD}^2 - r_{ID}^2))} \right)} \Leftrightarrow \Delta I_x = \frac{\Delta E_x}{R_5}$$

$$\Rightarrow \Delta I_m = \frac{\Delta E_x}{R_5} \cosh(\alpha(L - x))$$

The idea of this study was to demonstrate the ability to monitor a CP system through the ILI tool. In a real world example of an effective CP system, the current density will help to control calcareous deposit, which is developed over time and thus also controls the potential in the pipe-to-soil interface. Calcareous deposit can reduce current by increasing the resistivity of the coating, which is what this research is showing.

The other way to reduce current is by slowing the diffusion of oxygen through the coating to the steel surface. Anywhere the pipeline is poorly protected and the current density becomes so low far away from the rectifier is also where calcareous deposit will be lacking. “This would also work since calcareous deposit would change the diffusion Equation by decreasing the rate of diffusion constant over an increasing distance, Equation 1.7, causing the concentration gradient to decline by the denominator as the diffusion Equation increases.”²⁴

Finally, the current prediction from the attenuation model¹ implies that it is the maximum that can be provided by the CP system and NOT the actual current. The calcareous deposit effect remains the same, but it does not create the flat current effect, it just increases the range where potential and current are independent.

4.4. FUTURE WORK

There are many topics that this research immediately branches into with respect to the CP circuit potential, current, and the chemical interactions with the soil. As geometry of pipes change, temperature, and metal alloys may differ etc., these are useful additional

parameters for input into the model to establish more trends and make analyses. With additional samples more accurate trends could be established, especially with varying conditions (recall Section 2.2 for industry specific variances). Field tests would be useful to get potentials experimentally from CP coupons or test lead stations to further confirm specific aspects of Kirchhoff's methods as well as the attenuation models since it assumes a maximum current density.

4.4.1. Calcareous Deposit. Kinetic studies would be interesting to explore to determine how long it takes for a pipeline to become fully protected (polarized) and gain calcareous deposit. Mathematically, current density (flux) can be set up as a rate based on the unit relationships $W/m^2 = J/sec \cdot m^2$, where Amps = Watts/Volts, so $J/sec = Amps/Volt$, then seconds (time) = Volts*Joules/Amps.

A relationship between attenuation and wave propagation of the current may be established as well. This can be tied to the CP ILI tool current density readings, such that a time can be calculated and then validated by some known pipeline ages and upon excavating the pipe to observe coating condition and evidence of calcareous deposit.

4.4.2. Kirchhoff's Theory Applications. Field measurements are suggested to be gathered from CP coupons, test stations along a pipeline's CP system, and from the CP ILI tool regarding experimenting with applications of Kirchhoff's Method as outlined in Section 2.6. This additional research may help further validate methods from Section 2.4, ATTENUATION and provide new assessment techniques for evaluating CP systems relating to the CP ILI tool.

4.4.3. Diffusion Rate Experiments. This possible future research is in regards to Fick's Law, Equations (1.7) and (1.8), which is dependent upon the diffusion coefficient

D and the activation energy potential E for the diffusion process to occur in addition to the kinetic effects (rate of diffusion). The diffusivity constant (D) is a function of temperature T as well, where in industry and experimentally, the temperature can impact the diffusion rate. Experiments for diffusion based on temperature variation may further establish relationships with respect to the demand of current capacity for oxygen diffusion. A study like this can be compared to CP ILI measurement data to support whether or not oxygen is migrating to the surface or is no longer consumed by current. This study could expand upon to Figures 1.2, 1.3 and 4.1.

4.4.4. Noise and Vibration Filter. Other research may direct experts to seek solutions to cool down sensors that experience greater heat due to friction inside of dry gas lines. Dampening effects can be studied to reduce vibration by from more viscous fluids or alternative mechanics for the sensors. Alternatively data analysis and noise filtration built into a software program may help to estimate an average density.

4.4.5. Sensor Types and Arrangements. Additional studies may lead to different sensor arrangements such that contact methods may not be necessary. Sensor orientation for the tool considering ability to cover larger spans of area with smaller discrete areas to help normalize readings –like a blanket of sensors around the tool (i.e., the more samples the more accurate the reading).

4.4.6. Non-Surface-Contact Sensors. Fluid mechanics can be explored to help find the thermal circuitry via heat and mass transfer through the medium (fluid) in order to capture readings without making direct contact with the pipe by examining the heat flux which is basically current density as established through electromagnetism (Maxwell's Equations and the permeability and permittivity of the medium).

APPENDIX A.
MISCELLANEOUS TABLES & MATERIALS

A. MISCELLANEOUS TABLES & MATERIALS

Table of Soil Resistivity

Complimentary of Department of the Army; TM 5-811-7
Electrical Design, Cathodic Protection (1985)

Table 2-1. Corrosivity of soils on steel based on soil resistivity

Soil resistivity range (ohm-cm)	Corrosivity
0 to 2000	Severe
2000 to 10,000	Moderate to severe
10,000 to 30,000	Mild
Above 30,000	Not likely

U.S. Air Force.

Table 2-2. Typical current density requirements for cathodic protection of uncoated steel

Environment	Current density (mA/sq ft)	
	AFM 88-9 ^a	Ger ^{rard} ₈
Neutral soil	0.4 to 1.5	0.4 to 1.5
Well aerated neutral soil	2 to 3	2 to 3
Wet soil	1 to 6	2.5 to 6
Highly acidic soil	3 to 15	5 to 15
Soil supporting active sulfate-reducing bacteria	6 to 42	Up to 42
Heated soil	3 to 25	5 to 25
Stationary freshwater	1 to 6	5
Moving freshwater containing dissolved oxygen	5 to 15	5 to 15
Seawater	3 to 10	5 to 25

^aData are from Air Force Manual AFM 88-9, *Corrosion Control* (U.S. Air Force, August 1962), chap 4, p 203.

^rData are from J.S. Gerrard, "Practical Applications of Cathodic Protection," *Corrosion*, Vol 2 (L.L. Shreir, Ed.), Newnes-Butterworths, London, 1976, p 11:65. Used with permission.

Table of Steel Pipe Resistance – Some Standard Pipe Sizes
Complimentary of UFC 3-570-06; (2003)

Table 7-4. Estimated Resistance of Steel Pipelines

Nominal Pipeline Size (inches)	Outside Diameter (inches)	Wall Thickness (inches)	Weight per Foot (pounds)	Resistance per Foot (micro ohms)
2	2.375	0.154	3.65	79.20
4	4.500	0.237	10.80	26.80
6	6.625	0.280	19.00	15.20
8	8.625	0.322	28.60	10.10
10	10.750	0.365	40.50	7.13
12	12.750	0.375	49.60	5.82
14	14.000	0.375	54.60	5.29
16	16.000	0.375	62.60	4.61
18	18.00	0.375	70.60	4.09
20	20.000	0.375	78.60	3.68
22	22.000	0.375	86.60	3.34
24	24.000	0.375	94.60	3.06
26	26.000	0.375	102.60	2.82
28	28.000	0.375	110.60	2.62
30	30.000	0.375	118.70	2.44
32	32.000	0.375	126.60	2.28
34	34.000	0.375	134.60	2.15
36	36.000	0.375	142.60	2.03

Table of coating efficiencies from ²¹

Potential Variation in the Soil Around
a Pipe Calculated Following Reference ²¹

η_c , Coating Efficiency	$i_{avg} = (1 - \eta_c)i_{cathodic}$ mA/ft ²	$\Delta\phi$, V	$\kappa \Delta\phi / i_{avg} r_p$	Anode to Pipe Separation, ft	Consistent with Experiment ^a
99.9%	0.001	0.350	118	<0.4	Yes (holiday-free)
99.9%	0.01	0.350	11.8	<0.4	—
97.5%	0.025	0.350	4.74	<0.4	No (1 holiday)
97.5%	0.025	0.128	1.74	1.0	No (1 holiday)
97.5%	0.025	0.041	0.56	5.0	No (1 holiday)
95.0%	0.05	0.350	2.371	0.6	—
90.0%	0.10	0.350	1.185	2.1	—
80.0%	0.20	0.350	0.593	4.5	—
75.0%	0.25	0.350	0.474	6.0	—

^aUnder the assumption that holidays reduce the effective coating efficiency.

^b $i_{cathodic} = 10.7 \text{ mA/m}^2$ (1 mA/ft²), $r_p = 25.4 \text{ cm}$ (10 in.), $r_a = 1.27 \text{ cm}$ (0.5 in.), $\kappa = 9.26 \times 10^{-6} \text{ ohm}^{-1} \text{ cm}^{-1}$.

This table is from Lazzari and Pedferri¹

3.7 Summary of Protection Current Densities

Table 3.2 summarises protection current densities used in CP applications.

Environment	Protection current density (mA/m ²)
Soil	30 - 150
Neutral well aerated (sandy soil)	20 - 50
Acid water saturated soil	2 - 20
Water saturated (clayey soil)	50 - 450
Anaerobic (presence of SRB)	50 - 80
Hot pipelines	
Concrete	
Dry	2 - 20
Water saturated	0.2 - 2
Water (general)	$i_p = 4FD(O_2) \frac{Sb}{\phi}$ (see text)
Water	
Stagnant	$i_{p,s} \approx C(O_2)$; $[O_2]$ (ppm); $C = 8-10$
Flowing (laminar)	$i \approx i_{p,s}(1 + \sqrt{v})$; $v = \text{velocity (m/s)}$
Flowing (turbulent)	$i \approx i_{p,s}(1 + 0.5v)$; $v = \text{velocity (m/s)}$
Fresh water	
Stagnant	30 - 50
Flowing (laminar)	50 - 85
Flowing (turbulent)	50 - 160
Sea water	
Stagnant	50 - 110
Flowing (laminar)	60 - 140
Flowing (turbulent)	80 - 550
Condensers, Heat exchangers	100 - 1,300
Hot risers	120 - 600
Acids	50 - 1,500
Coated steel	
Soil	0.01 - 1
Sea water	0.1 - 10

APPENDIX B.
LITERATURE & PATENT REVIEW

B. LITERATURE & PATENT REVIEW

Research material for developing this thesis consisted of reviewing the patented CP ILI tool's data provided by BHI and cooperative efforts for data analyses by industry subject matter experts, publications (articles), consultations with the owners and designers of the tool about ideas for conceptualizing tool results via mathematical models. Articles, industry standards, and texts for CP design, its purpose and industry rules (regulations) for its maintenance and effectiveness were referenced and cited. The applied physics necessary for the analysis in Section 2 required general foundational concepts from engineering and science text books with respect to electrochemistry, general circuitry, materials and metallurgy were also referenced as applicable to achieve a valid analysis. The entire contents of this thesis was reviewed, collaborated, and vetted by industry SMEs, Professors, and mentors.

The following listed patent information, general publications, and subject matter experts' knowledge and experience was utilized:

- CP ILI Tool™, Patent No. 7,104,147, Sept. 2006
 - Inventors: Pots; Bert (Houston, TX), Fagbayi; Kola (Houston, TX), Scott; P. Kevin (Harvey, LA), Mateer; Mark W. (Katy, TX)
 - Assignee: Shell Oil Company (Houston, TX) Family ID: 34807922
 - Appl. No.: 10/768,618
 - Filed: January 30, 2004
 - CP ILI tool—is designed by Baker Hughes and in their ownership
- Baker Hughes Incorporated (CP ILI Tool™ owner) – Dennis Janda and David Williams provided SME knowledge of tool use, design, 12” OD & 0.5” std w.t.

data, CP ILI data, and performance, mentorship, guidance, interviews, collaborations, publications, concepts for research, and thesis review.

- Military –Various Army and Navy article publications and standards for designs and for CP of submerged metallic structures, tanks, and pipelines and corrosion prevention.
- Missouri University of Science & Technology – PhD. Engineering Professors:
 - Matt J. O’Keefe (co-advisor) –metallurgy, coatings and corrosion expert;
 - Victor Birman (co-advisor) – materials and composites expert; and
 - James L. Drewniak (committee member) – electrical engineering expert;

These engineering experts provided guidance, publications on material, mentorship, and directions for adhering to thesis criteria and authorizations for acceptance of real work thesis material in accordance to University processes, procedures, and in order to complete the thesis paper and presentation requirements.
- Industry Expert from Shell Corporation –Principle Corrosion, CP, and System Integrity Mark Mateer, provided SME guidance, mentorship, interviews, publications, text books, and help with honing thesis approach as well as complete review for all of the thesis paper with respect to validity of CP, corrosion concepts, system integrity, and methodology for analyses.
- Industry Expert from Technical Toolboxes – Corrosion, CP, and System Integrity Expert: Joe Pikas, provided SME guidance, mentorship, publications, review of thesis material, and concepts for approach.
- Text books, articles (publications); (see Section 5.2 and BIBLIOGRAPHY)

APPENDIX C.

OTHER REFERENCES & MATERIAL

C. OTHER REFERENCES & MATERIAL

Electronic Code of Federal Regulations (e-CFR) (2016), *Title 49 (Transportation)*
 “Pipeline and Hazardous Materials Safety Administration, Department of
 Transportation.” website <http://www.ecfr.gov/cgi-bin/text-idx?tpl=%2Findex.tpl>.

- a. Part 192 – Transportaion of Natural and Other Gas by Pipeline: Minimum Federal Safety Standard; Subpart I §192.463-.475
- b. Part 195 – Transportation of Hazardous Liquids by Pipeline; Subpart H §195.557, .563 & .565.

Incropera, F. P. & DeWitt, P.D. (2002). *Heat and Mass Transfer, Fifth Edition*.
 Hoboken, NJ: John Wiley & Sons, Inc.

Janda, D.; Williams, D. (2014). “Countering Sleepless Nights.” World of Pipelines & Baker Hughes: Houston, TX.

Janda, D.; Williams, D. (2014). “Lessons Learned: Monitoring Cathodic Protection from Inside the Pipe,” *Materials Performance*, pages 42-45.

NACE International SP0169-2007 Standard Practice (formerly RP0169, recommended practice), (2007). "Control of External Corrosion on Underground or Submerged Metallic Piping Systems." NACE: Houston, TX.

NACE SP0502 Standard Practice3 – “Pipeline External Corrosion Direct Assessment”, (NACE ECDA (DA)).

O’Keefe, M. J.; Drewniak, J.L.; Maddela, S.; Claypook, J. & Fang, X. (2014).

"Development of an Alternative Method to Potential Measurement to Assess the Level of Cathodic Protection to a Buried or Submerged Pipeline" PRCI on behalf of Technical Toolboxes, Inc., Houston, TX.

Orazem, M. E.; Qiu, C. (2002). "Model for Interpretation of Pipeline Survey Data",
Univeristy of Florida, Technical Toolboxes, Inc., Houston, TX. (Close Interval Survey
related)

Peabody, A.W. (2001). "Control of Pipeline Corrosion", 2nd Edition. p. 19. R.
Bianchetti, NACE: Houston, TX.

BIBLIOGRAPHY

- [1] Lazzari, L.; Pedferri, P. (2006); “Cathodic protection” (1st Edition). Polipress, Politecnico di Milano Piazza Leonardo da Vinci, 32-20133 Milano.
- [2] Department of Defence (2003). *Operation and Maintenance: Cathodic Protection*. UFC-3-570-06, Chapter 2-1 (Corrosion Cell), CP Design.
- [3] Mateer, M. (2017, April 10). *Background on Corrosion and CP, CP ILI Data Analysis Approach* [Telephone interview #1]. Discussions with Mark Mateer, Principal Asset Integrity Engineer.
- [4] Kotz, J.; Treichel, P.; (1999) “Chemistry and Chemical Reactivity, Fourth Edition” (Gibbs Free Energy, Standard Potentials, and Electrochemical Cells – Nernst Equation), Chapters: 21 and 20.3; Saunders College Publishing: Fort Worth, TX.
- [5] Kittel, C.; (2005), “Introduction to Solid State Physics, Eighth Edition” (Diffusion), Chapters: 20; John Wiley & Sons, Inc.: Hoboken, NJ.
- [6] Janda, D.; Williams, D. (2014). “Developing a Standardized Process for Cathodic Protection Current Measurement on In-Service Pipelines – Process and Procedures for a New Technology.” NACE & Baker Hughes: Houston, TX.
- [7] Mateer, M; Pikas, Joe, Williams, D.; (2017, April 03). *General agreed concept, throughout industry*. [General Correspondence] Discussions with industry SMEs from Shell, Technical Toolboxes, and BHI.
- [8] Williams, D. (2017, March 31). *Background on Corrosion, CP, CP ILI Data Analysis* [Telephone interview]. Discussions with David Williams (CP Specialist & NACE CP4 Certified at BHI).
- [9] Nicholson, J.P. (2011), “Pipeline Integrity, Pipeline Corrosion Control.” World of Pipelines, Cathodic Technology Ltd., CAN
- [10] Morgan, J. (1987); “Cathodic Protection” (2nd Edition). NACE, Houston TX, Chapter 2 and APPENDIX D.
- [11] Mateer, M.; (2017, April 3rd- 4th). *Background on Corrosion and CP, CP ILI Data Analysis Approach* [Telephone interview #2]. Discussions with Mark Mateer, Principal Asset Integrity Engineer.

- [12] Bash, R. (2011), "Observations From 56 Years Of Pipeline Corrosion Damage Excavations" Pipeline & Gas Journal, Volume 238, No.3; <https://pgjonline.com>
- [13] Pipeline Hazardous Material and Safety Administration (PHMSA) "Fact Sheet: Close Interval Survey", <http://primis.phmsa.dot.gov/comm/FactSheets/FSCloseInternalSurvey.htm>, 2017.
- [14] Janda, D.; Williams, D. (2010). "Inline Cathodic Protection Monitoring." World of Pipelines & Baker Hughes: Houston, TX
- [15] Janda, D.; Williams, D. (2014). "Developing a Standardized Process for Cathodic Protection Current Measurement on In-Service Pipelines – Process and Procedures for a New Technology." NACE & Baker Hughes: Houston, TX.
- [16] Pioneer Pipe (2014). "Standards and Specifications", 5th Edition 11. Houston, TX.
- [17] Griffiths, D.J. (1999). "Introduction to Electrodynamics," (Third Edition). Patparganj, Delhi 110 092, India: Pearson Education, Inc.
- [18] Headquarters, Department of the Army (1985). *Electrical Design, Cathodic Protection*. No. TM 5-811-7 (Technical Manual Submerged Structures), Chapter 1, Washington D.C.
- [19] Department of Defence (2003). *Operation and Maintenance: Cathodic Protection*. UFC-3-570-06, Chapter 2-1 (Corrosion Cell), CP Design.
- [20] Mateer, M. (2017, May 02). *CP ILI Data Analysis Approach* Telephone [Interview #3]. Discussions with Mark Mateer, Principal Asset Integrity Engineer
- [21] Orazem, M.E.; Kennelley, J.K.; Bone, L. (1993). "Current and Potential Distribution of a Coated Pipeline with Holidays, Part II – Comparison of the Effect of Discrete and Distributed Holidays", NACE Corrosion- Vol. 49, No.3.
- [22] Mateer, M., & Williams, D. (2017, May 02). CP ILI tool Data Plots. [Unpublished raw data]. Data from BHI; honed analytical process and approach by Mark Mateer.
- [23] Mateer, M. (2017, May 12). CP ILI Data Analysis Approach on Telephone [Interview #4]. Discussions with Mark Mateer, Principal Asset Integrity Engineer

- [24] Mateer, M. (2017, May 23-30). CP ILI Data Analysis Approach [Model Collaborations and Correspondence]. Discussions with Mark Mateer, Principal Asset Integrity Engineer
- [25] Allahar, Kerry N.; Orazem, Mark E. (2009) "On the Extension of CP Models to Address Cathodic Protection Under a Delaminated Surface." Elsevier Ltd., University of Florida: Gainesville, FL.

VITA

Briana Ley Ferguson was a full time professional student, while she completed her Bachelor of Science in Mechanical Engineering from University of Colorado, Colorado Springs in 2007 after completing two Associate of Science degrees in Drafting and Design. She gained a broad educational background with emphases in heat and mass transfer; thermodynamics; solid state materials physics (materials science); fluid dynamics (Newtonian and non-Newtonian); electrostatics; and magnetism.

With many years of direct industry experience in energy, oil, and gas, Briana has held various positions as a Drafter, Design Engineer, Project Engineer, Manager of Risk Engineering (Integrity), and a Lead Integrity and Compliance Engineer. The majority of her career has been in midstream (pipeline systems and facilities) with some upstream, downstream, maritime, and storage. As Integrity Engineering has multifaceted disciplines, she became interested and inspired by her mentors to acquire more specific and deeper knowledge about cathodic protection (CP) systems and the methods for proactively reducing external pipeline corrosion through CP measurement via inline inspection devices, hence completion of her Master of Science in Mechanical Engineering, thesis option, on the research topic “CP Measurement via ILI” in July, 2017 from Missouri University of Science and Technology.